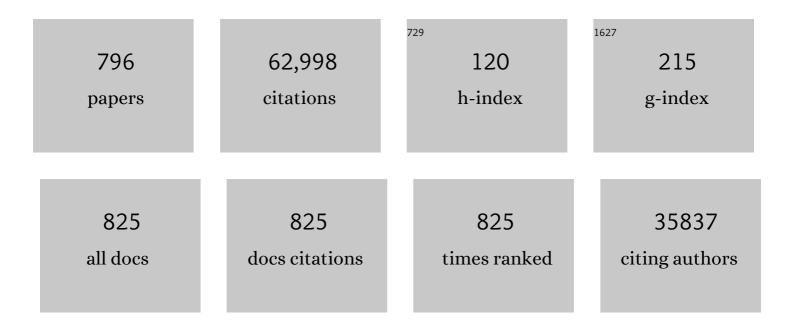
Licheng Sun

List of Publications by Year in descending order

Source: https://exaly.com/author-pdf/4560158/publications.pdf Version: 2024-02-01



#	Article	IF	CITATIONS
1	2D materials for solar fuels via artificial photosynthesis. National Science Review, 2022, 9, nwab116.	4.6	6
2	Isolation and Identification of Pseudo Seven-Coordinate Ru(III) Intermediate Completing the Catalytic Cycle of Ru-bda Type of Water Oxidation Catalysts. CCS Chemistry, 2022, 4, 2481-2490.	4.6	16
3	Highly stable perovskite solar cells with a novel Ni-based metal organic complex as dopant-free hole-transporting material. Journal of Energy Chemistry, 2022, 65, 312-318.	7.1	11
4	A Phenanthrocarbazoleâ€Based Dopantâ€Free Holeâ€Transport Polymer with Noncovalent Conformational Locking for Efficient Perovskite Solar Cells. Angewandte Chemie - International Edition, 2022, 61, .	7.2	47
5	In‣itu Generated CsPbBr ₃ Nanocrystals on Oâ€Defective WO ₃ for Photocatalytic CO ₂ Reduction. ChemSusChem, 2022, 15, .	3.6	33
6	Effect of the Ancillary Ligand on the Performance of Heteroleptic Cu(I) Diimine Complexes as Dyes in Dye-Sensitized Solar Cells. ACS Applied Energy Materials, 2022, 5, 1460-1470.	2.5	10
7	Efficient dye-sensitized solar cells based on bioinspired copper redox mediators by tailoring counterions. Journal of Materials Chemistry A, 2022, 10, 4131-4136.	5.2	4
8	WO ₃ Nanosheet-Supported IrW Alloy for High-Performance Acidic Overall Water Splitting with Low Ir Loading. ACS Applied Energy Materials, 2022, 5, 970-980.	2.5	15
9	Sacrificial W Facilitates Selfâ€Reconstruction with Abundant Active Sites for Water Oxidation. Small, 2022, 18, e2107249.	5.2	17
10	Natural Chlorophyll Derivative Assisted Defect Passivation and Hole Extraction for MAPbl ₃ Perovskite Solar Cells with Efficiency Exceeding 20%. ACS Applied Energy Materials, 2022, 5, 1390-1396.	2.5	5
11	Engineering MoO _{<i>x</i>} /MXene Hole Transfer Layers for Unexpected Boosting of Photoelectrochemical Water Oxidation. Angewandte Chemie - International Edition, 2022, 61, .	7.2	80
12	Photoelectrochemical water oxidation improved by pyridine <i>N</i> -oxide as a mimic of tyrosine-Z in photosystem II. Chemical Science, 2022, 13, 4955-4961.	3.7	4
13	Water oxidation by a noble metal-free photoanode modified with an organic dye and a molecular cobalt catalyst. Journal of Materials Chemistry A, 2022, 10, 9121-9128.	5.2	6
14	Pyreneâ€Based Dopantâ€Free Holeâ€Transport Polymers with Fluorineâ€Induced Favorable Molecular Stacking Enable Efficient Perovskite Solar Cells. Angewandte Chemie - International Edition, 2022, 61, .	7.2	31
15	Promoting Proton Transfer and Stabilizing Intermediates in Catalytic Water Oxidation via Hydrophobic Outer Sphere Interactions. Chemistry - A European Journal, 2022, 28, .	1.7	11
16	Polymeric Viologen-Based Electron Transfer Mediator for Improving the Photoelectrochemical Water Splitting on Sb2Se3 Photocathode. Fundamental Research, 2022, , .	1.6	0
17	Rubrene Nanoaggregate-Integrated CH ₃ NH ₃ PbI ₃ Bilayer Film: Role of Singlet Fission and Photon Upconversion. ACS Applied Nano Materials, 2022, 5, 801-809.	2.4	1
18	Promotion of the oxygen evolution performance of Ni-Fe layered hydroxides via the introduction of a proton-transfer mediator anion. Science China Chemistry, 2022, 65, 382-390.	4.2	20

#	Article	IF	CITATIONS
19	Enhancement of Singlet Fission Yield by Hindering Excimer Formation in Perylene Film. Journal of Physical Chemistry C, 2022, 126, 396-403.	1.5	13
20	NiCo ₂ O ₄ thin film prepared by electrochemical deposition as a hole-transport layer for efficient inverted perovskite solar cells. RSC Advances, 2022, 12, 12544-12551.	1.7	3
21	Triggering Lattice Oxygen Activation of Singleâ€Atomic Mo Sites Anchored on Ni–Fe Oxyhydroxides Nanoarrays for Electrochemical Water Oxidation. Advanced Materials, 2022, 34, e2202523.	11.1	103
22	Intramolecular hydroxyl nucleophilic attack pathway by a polymeric water oxidation catalyst with single cobalt sites. Nature Catalysis, 2022, 5, 414-429.	16.1	85
23	Multiphase Fluid Dynamics and Mass Transport Modeling in a Porous Electrode toward Hydrogen Evolution Reaction. Industrial & Engineering Chemistry Research, 2022, 61, 8323-8332.	1.8	5
24	Regulating *OCHO Intermediate as Rateâ€Đetermining Step of Defective Oxynitride Nanosheets Enabling Robust CO ₂ Electroreduction. Advanced Energy Materials, 2022, 12, .	10.2	32
25	Reversible Structural Isomerization of Nature's Water Oxidation Catalyst Prior to O–O Bond Formation. Journal of the American Chemical Society, 2022, 144, 11736-11747.	6.6	15
26	The future challenges in molecular water oxidation catalysts. Journal of Energy Chemistry, 2022, 73, 643-645.	7.1	1
27	Progress of Experimental and Computational Catalyst Design for Electrochemical Nitrogen Fixation. ACS Catalysis, 2022, 12, 8936-8975.	5.5	41
28	A crosslinked polymer as dopant-free hole-transport material for efficient n-i-p type perovskite solar cells. Journal of Energy Chemistry, 2021, 55, 211-218.	7.1	29
29	Switching O O bond formation mechanism between WNA and I2M pathways by modifying the Ru-bda backbone ligands of water-oxidation catalysts. Journal of Energy Chemistry, 2021, 54, 815-821.	7.1	16
30	A Cobalt@Cucurbit[5]uril Complex as a Highly Efficient Supramolecular Catalyst for Electrochemical and Photoelectrochemical Water Splitting. Angewandte Chemie, 2021, 133, 2004-2013.	1.6	18
31	Tuning the O–O bond formation pathways of molecular water oxidation catalysts on electrode surfaces via second coordination sphere engineering. Chinese Journal of Catalysis, 2021, 42, 460-469.	6.9	7
32	Revealing ultrafast relaxation dynamics in six-thiophene thin film and single crystal. Journal of Photochemistry and Photobiology A: Chemistry, 2021, 404, 112920.	2.0	6
33	A Cobalt@Cucurbit[5]uril Complex as a Highly Efficient Supramolecular Catalyst for Electrochemical and Photoelectrochemical Water Splitting. Angewandte Chemie - International Edition, 2021, 60, 1976-1985.	7.2	55
34	Necessity of structural rearrangements for O O bond formation between O5 and W2 in photosystem II. Journal of Energy Chemistry, 2021, 57, 436-442.	7.1	7
35	<i>N</i> -Bromosuccinimide as a p-type dopant for a Spiro-OMeTAD hole transport material to enhance the performance of perovskite solar cells. Sustainable Energy and Fuels, 2021, 5, 2294-2300.	2.5	5
36	From Ru-bda to Ru-bds: a step forward to highly efficient molecular water oxidation electrocatalysts under acidic and neutral conditions. Nature Communications, 2021, 12, 373.	5.8	37

#	Article	IF	CITATIONS
37	Metal–organic frameworks and their derivatives as electrocatalysts for the oxygen evolution reaction. Chemical Society Reviews, 2021, 50, 2663-2695.	18.7	333
38	In Situ Induced Crystalline–Amorphous Heterophase Junction by K+ to Improve Photoelectrochemical Water Oxidation of BiVO4. ACS Applied Materials & Interfaces, 2021, 13, 2723-2733.	4.0	10
39	Selective Electrochemical Alkaline Seawater Oxidation Catalyzed by Cobalt Carbonate Hydroxide Nanorod Arrays with Sequential Proton-Electron Transfer Properties. ACS Sustainable Chemistry and Engineering, 2021, 9, 905-913.	3.2	25
40	Surface and bulk reconstruction of CoW sulfides during pH-universal electrocatalytic hydrogen evolution. Journal of Materials Chemistry A, 2021, 9, 11359-11369.	5.2	21
41	Ultrafast spectroscopy reveals singlet fission, ionization and excimer formation in perylene film. Scientific Reports, 2021, 11, 5220.	1.6	26
42	Switching the O-O Bond Formation Pathways of Ru-pda Water Oxidation Catalyst by Third Coordination Sphere Engineering. Research, 2021, 2021, 9851231.	2.8	7
43	Helical Copper Redox Mediator with Low Electron Recombination for Dye-Sensitized Solar Cells. ACS Sustainable Chemistry and Engineering, 2021, 9, 5252-5259.	3.2	6
44	Offâ€Set Interactions of Ruthenium–bda Type Catalysts for Promoting Waterâ€Splitting Performance. Angewandte Chemie, 2021, 133, 14625-14632.	1.6	5
45	Thiophene-fused carbazole derivative dyes for high-performance dye-sensitized solar cells. Tetrahedron, 2021, 88, 132124.	1.0	5
46	Offâ€Set Interactions of Ruthenium–bda Type Catalysts for Promoting Waterâ€Splitting Performance. Angewandte Chemie - International Edition, 2021, 60, 14504-14511.	7.2	13
47	Conformal Macroporous Inverse Opal Oxynitride-Based Photoanode for Robust Photoelectrochemical Water Splitting. Journal of the American Chemical Society, 2021, 143, 7402-7413.	6.6	76
48	Ni III â€rich NiFeBa as an Efficient Catalyst for Water Oxidation. ChemSusChem, 2021, 14, 2516-2520.	3.6	2
49	Metalloid Teâ€Doped Feâ€Based Catalysts Applied for Electrochemical Water Oxidation. ChemistrySelect, 2021, 6, 6154-6158.	0.7	7
50	Stable Dye‧ensitized Solar Cells Based on Copper(II/I) Redox Mediators Bearing a Pentadentate Ligand. Angewandte Chemie, 2021, 133, 16292-16299.	1.6	6
51	Stable Dye‣ensitized Solar Cells Based on Copper(II/I) Redox Mediators Bearing a Pentadentate Ligand. Angewandte Chemie - International Edition, 2021, 60, 16156-16163.	7.2	24
52	Engineering single-atomic ruthenium catalytic sites on defective nickel-iron layered double hydroxide for overall water splitting. Nature Communications, 2021, 12, 4587.	5.8	401
53	Hydrophobic Interactions of Ru-bda-Type Catalysts for Promoting Water Oxidation Activity. Energy & Fuels, 2021, 35, 19096-19103.	2.5	7
54	Identification of Mâ€NH 2 â€NH 2 Intermediate and Rate Determining Step for Nitrogen Reduction with Bioinspired Sulfurâ€Bonded FeW Catalyst. Angewandte Chemie, 2021, 133, 20494-20504.	1.6	11

#	Article	IF	CITATIONS
55	Molecular Engineering of Photocathodes based on Polythiophene Organic Semiconductors for Photoelectrochemical Hydrogen Generation. ACS Applied Materials & Interfaces, 2021, 13, 40602-40611.	4.0	8
56	Selective Electro-oxidation of Alcohols to the Corresponding Aldehydes in Aqueous Solution via Cu(III) Intermediates from CuO Nanorods. ACS Sustainable Chemistry and Engineering, 2021, 9, 11855-11861.	3.2	19
57	Singlet Fission, Polaron Formation, and Energy Transfer in Indolo[3,2-b]carbazole Thin Films and Single Crystals. Journal of Physical Chemistry C, 2021, 125, 18827-18833.	1.5	2
58	Identification of Mâ€NH ₂ â€NH ₂ Intermediate and Rate Determining Step for Nitrogen Reduction with Bioinspired Sulfurâ€Bonded FeW Catalyst. Angewandte Chemie - International Edition, 2021, 60, 20331-20341.	7.2	65
59	Dye-sensitized photoanode decorated with pyridine additives for efficient solar water oxidation. Chinese Journal of Catalysis, 2021, 42, 1352-1359.	6.9	8
60	Numerical investigation and comparative analysis of nanofluid cooling enhancement for TEG and TEC systems. Case Studies in Thermal Engineering, 2021, 27, 101331.	2.8	23
61	Supramolecular Co-adsorption on TiO ₂ to enhance the efficiency of dye-sensitized solar cells. Journal of Materials Chemistry A, 2021, 9, 13697-13703.	5.2	5
62	Remarkable synergy of borate and interfacial hole transporter on BiVO ₄ photoanodes for photoelectrochemical water oxidation. Materials Advances, 2021, 2, 4323-4332.	2.6	12
63	Bio-Inspired Water Oxidation Catalysts. , 2021, , 589-610.		0
64	Singlet fission from upper excited singlet states and polaron formation in rubrene film. RSC Advances, 2021, 11, 4639-4645.	1.7	15
65	Investigation on the Extendibility of Self-Similar Heat Sink for Cooling Electrical Equipment With Varying Sizes. IEEE Transactions on Components, Packaging and Manufacturing Technology, 2021, 11, 57-70.	1.4	2
66	Electronic Influence of the 2,2′-Bipyridine-6,6′-dicarboxylate Ligand in Ru-Based Molecular Water Oxidation Catalysts. Inorganic Chemistry, 2021, 60, 1202-1207.	1.9	10
67	Engineering Lattice Oxygen Activation of Iridium Clusters Stabilized on Amorphous Bimetal Borides Array for Oxygen Evolution Reaction. Angewandte Chemie - International Edition, 2021, 60, 27126-27134.	7.2	106
68	Exploration of electrocatalytic water oxidation properties of NiFe catalysts doped with nonmetallic elements (P, S, Se). International Journal of Hydrogen Energy, 2021, 46, 38992-39002.	3.8	10
69	Towards efficient photochemistry from upper excited electronic states: detection of long S2 lifetime of perylene. Journal of Chemical Physics, 2021, 155, 191102.	1.2	3
70	Engineering Lattice Oxygen Activation of Iridium Clusters Stabilized on Amorphous Bimetal Borides Array for Oxygen Evolution Reaction. Angewandte Chemie, 2021, 133, 27332-27340.	1.6	6
71	Two-Dimensional Defective Boron-Doped Niobic Acid Nanosheets for Robust Nitrogen Photofixation. ACS Nano, 2021, 15, 17820-17830.	7.3	26
72	Engineering Single-Atomic Ni-N ₄ -O Sites on Semiconductor Photoanodes for High-Performance Photoelectrochemical Water Splitting. Journal of the American Chemical Society, 2021, 143, 20657-20669.	6.6	114

#	Article	IF	CITATIONS
73	Switching Pathways of Triplet State Formation by Twisted Intramolecular Charge Transfer. Journal of Physical Chemistry B, 2021, 125, 12518-12527.	1.2	6
74	An investigation on the performance of a micro-scale Venturi bubble generator. Chemical Engineering Journal, 2020, 386, 120980.	6.6	40
75	Electronâ€Withdrawing Anchor Group of Sensitizer for Dyeâ€&ensitized Solar Cells, Cyanoacrylic Acid, or Benzoic Acid?. Solar Rrl, 2020, 4, 1900436.	3.1	20
76	Defect Engineering of Photocatalysts for Solar Energy Conversion. Solar Rrl, 2020, 4, 1900487.	3.1	85
77	Amorphous WO ₃ induced lattice distortion for a low-cost and high-efficient electrocatalyst for overall water splitting in acid. Sustainable Energy and Fuels, 2020, 4, 1712-1722.	2.5	14
78	The application of transition metal complexes in hole-transporting layers for perovskite solar cells: Recent progress and future perspectives. Coordination Chemistry Reviews, 2020, 406, 213143.	9.5	50
79	Hierarchical micro-reactor as electrodes for water splitting by metal rod tipped carbon nanocapsule self-assembly in carbonized wood. Applied Catalysis B: Environmental, 2020, 264, 118536.	10.8	25
80	Selectively Etching Vanadium Oxide to Modulate Surface Vacancies of Unary Metal–Based Electrocatalysts for Highâ€₽erformance Water Oxidation. Advanced Energy Materials, 2020, 10, 1903571.	10.2	64
81	3D Porous Pyramid Heterostructure Array Realizing Efficient Photoâ€Electrochemical Performance. Advanced Energy Materials, 2020, 10, 1902935.	10.2	41
82	Molybdenum and boron synergistically boosting efficient electrochemical nitrogen fixation. Nano Energy, 2020, 78, 105391.	8.2	21
83	Molecular Functionalization of NiO Nanocatalyst for Enhanced Water Oxidation by Electronic Structure Engineering. ChemSusChem, 2020, 13, 5901-5909.	3.6	14
84	Beyond d Orbits: Steering the Selectivity of Electrochemical CO ₂ Reduction via Hybridized sp Band of Sulfurâ€Incorporated Porous Cd Architectures with Dual Collaborative Sites. Advanced Energy Materials, 2020, 10, 2002499.	10.2	20
85	Fine-Tuning by Triple Bond of Carbazole Derivative Dyes to Obtain High Efficiency for Dye-Sensitized Solar Cells with Copper Electrolyte. ACS Applied Materials & Interfaces, 2020, 12, 46397-46405.	4.0	27
86	Unveiling the light soaking effects of the CsPbI3 perovskite solar cells. Journal of Power Sources, 2020, 472, 228506.	4.0	21
87	Boosting Electrocatalytic Water Oxidation by Creating Defects and Latticeâ€Oxygen Active Sites on Niâ€Fe Nanosheets. ChemSusChem, 2020, 13, 5067-5072.	3.6	12
88	Cobalt doped BiVO ₄ with rich oxygen vacancies for efficient photoelectrochemical water oxidation. RSC Advances, 2020, 10, 28523-28526.	1.7	22
89	Nickel-selenide templated binary metal–organic frameworks for efficient water oxidation. Journal of Materials Chemistry A, 2020, 8, 16908-16912.	5.2	31
90	Enrichment of glycopeptides using environmentally friendly wood materials. Green Chemistry, 2020, 22, 5666-5676.	4.6	24

#	Article	IF	CITATIONS
91	A dendritic Sb ₂ Se ₃ /In ₂ S ₃ heterojunction nanorod array photocathode decorated with a MoS _x catalyst for efficient solar hydrogen evolution. Journal of Materials Chemistry A, 2020, 8, 23385-23394.	5.2	21
92	Engineering active sites on hierarchical transition bimetal oxides/sulfides heterostructure array enabling robust overall water splitting. Nature Communications, 2020, 11, 5462.	5.8	383
93	Metal–Molybdenum Sulfide Nanosheet Arrays Prepared by Anion Exchange as Catalysts for Hydrogen Evolution. Energy Technology, 2020, 8, 2000595.	1.8	2
94	Conformational and Compositional Tuning of Phenanthrocarbazole-Based Dopant-Free Hole-Transport Polymers Boosting the Performance of Perovskite Solar Cells. Journal of the American Chemical Society, 2020, 142, 17681-17692.	6.6	83
95	Stabilization of a molecular water oxidation catalyst on a dyeâ^'sensitized photoanode by aÂpyridyl anchor. Nature Communications, 2020, 11, 4610.	5.8	38
96	Selective CO Production by Photoelectrochemical CO ₂ Reduction in an Aqueous Solution with Cobalt-Based Molecular Redox Catalysts. ACS Applied Materials & Interfaces, 2020, 12, 41644-41648.	4.0	13
97	Editorial for the Special Issue of ChemSusChem on Green Carbon Science: CO 2 Capture and Conversion. ChemSusChem, 2020, 13, 6051-6053.	3.6	0
98	Triazatruxene-based sensitizers for highly efficient solid-state dye-sensitized solar cells. Solar Energy, 2020, 212, 1-5.	2.9	9
99	Magnetizing lead-free halide double perovskites. Science Advances, 2020, 6, .	4.7	56
100	Upper Excited State Photophysics of Malachite Green in Solution and Films. Journal of Physical Chemistry B, 2020, 124, 4293-4302.	1.2	5
101	Ionic liquid doped organic hole transporting material for efficient and stable perovskite solar cells. Physica B: Condensed Matter, 2020, 586, 412124.	1.3	18
102	Ultrafast Tuning of Various Photochemical Pathways in Perylene–TCNQ Charge-Transfer Crystals. Journal of Physical Chemistry C, 2020, 124, 13894-13901.	1.5	13
103	Side-chain engineering of PEDOT derivatives as dopant-free hole-transporting materials for efficient and stable n–i–p structured perovskite solar cells. Journal of Materials Chemistry C, 2020, 8, 9236-9242.	2.7	14
104	Urchinâ€Like Cobaltâ€Copper (Hydr)oxides as an Efficient Water Oxidation Electrocatalyst. ChemPlusChem, 2020, 85, 1339-1346.	1.3	7
105	Top-Down Approach Making Anisotropic Cellulose Aerogels as Universal Substrates for Multifunctionalization. ACS Nano, 2020, 14, 7111-7120.	7.3	147
106	Copper Selenide–Derived Copper Oxide Nanoplates as a Durable and Efficient Electrocatalyst for Oxygen Evolution Reaction. Energy Technology, 2020, 8, 2000142.	1.8	14
107	Organic Salts as p-Type Dopants for Efficient LiTFSI-Free Perovskite Solar Cells. ACS Applied Materials & Interfaces, 2020, 12, 33751-33758.	4.0	24
108	Advancing Proton Exchange Membrane Electrolyzers with Molecular Catalysts. Joule, 2020, 4, 1408-1444.	11.7	35

#	Article	IF	CITATIONS
109	Promoting the Fe(VI) active species generation by structural and electronic modulation of efficient iron oxide based water oxidation catalyst without Ni or Co. Nano Energy, 2020, 72, 104656.	8.2	35
110	Electroless Plating of NiFeP Alloy on the Surface of Silicon Photoanode for Efficient Photoelectrochemical Water Oxidation. ACS Applied Materials & Interfaces, 2020, 12, 11479-11488.	4.0	28
111	Single crystal structure and opto-electronic properties of oxidized Spiro-OMeTAD. Chemical Communications, 2020, 56, 1589-1592.	2.2	24
112	Copper-based homogeneous and heterogeneous catalysts for electrochemical water oxidation. Nanoscale, 2020, 12, 4187-4218.	2.8	79
113	Homogeneous Electrochemical Water Oxidation at Neutral pH by Waterâ€Soluble Ni ^{II} Complexes Bearing Redox Nonâ€innocent Tetraamido Macrocyclic Ligands. ChemSusChem, 2020, 13, 3277-3282.	3.6	30
114	Electrocatalytic Hydrogenation and Oxidation in Aqueous Conditions ^{â€} . Chinese Journal of Chemistry, 2020, 38, 996-1004.	2.6	38
115	Hydrophobic/Hydrophilic Directionality Affects the Mechanism of Ru-Catalyzed Water Oxidation Reaction. ACS Catalysis, 2020, 10, 13364-13370.	5.5	15
116	Electrochemical and photoelectrochemical water splitting with a CoOx catalyst prepared by flame assisted deposition. Dalton Transactions, 2020, 49, 588-592.	1.6	3
117	An organic polymer CuPPc-derived copper oxide as a highly efficient electrocatalyst for water oxidation. Chemical Communications, 2020, 56, 3797-3800.	2.2	9
118	High isotropic dispiro structure hole transporting materials for planar perovskite solar cells. Journal of Energy Chemistry, 2019, 32, 152-158.	7.1	7
119	Enhanced performance of perovskite solar cells using p-type doped PFB:F4TCNQ composite as hole transport layer. Journal of Alloys and Compounds, 2019, 771, 25-32.	2.8	19
120	Impact of Linking Topology on the Properties of Carbazoleâ€Based Holeâ€Transport Materials and their Application in Solidâ€State Mesoscopic Solar Cells. Solar Rrl, 2019, 3, 1900196.	3.1	17
121	Exploring Overall Photoelectric Applications by Organic Materials Containing Symmetric Donor Isomers. Chemistry of Materials, 2019, 31, 8810-8819.	3.2	12
122	Efficient BiVO ₄ Photoanodes by Postsynthetic Treatment: Remarkable Improvements in Photoelectrochemical Performance from Facile Borate Modification. Angewandte Chemie - International Edition, 2019, 58, 19027-19033.	7.2	108
123	Highly transparent nickel and iron sulfide on nitrogen-doped carbon films as counter electrodes for bifacial quantum dot sensitized solar cells. Solar Energy, 2019, 193, 766-773.	2.9	15
124	A bio-inspired coordination polymer as outstanding water oxidation catalyst via second coordination sphere engineering. Nature Communications, 2019, 10, 5074.	5.8	203
125	Efficient BiVO ₄ Photoanodes by Postsynthetic Treatment: Remarkable Improvements in Photoelectrochemical Performance from Facile Borate Modification. Angewandte Chemie, 2019, 131, 19203-19209.	1.6	35
126	The Central Role of Ligand Conjugation for Properties of Coordination Complexes as Hole-Transport Materials in Perovskite Solar Cells. ACS Applied Energy Materials, 2019, 2, 6768-6779.	2.5	11

#	Article	IF	CITATIONS
127	Exploring the Optical and Electrochemical Properties of Homoleptic versus Heteroleptic Diimine Copper(I) Complexes. Inorganic Chemistry, 2019, 58, 12167-12177.	1.9	25
128	Hierarchical CoS ₂ /Ni ₃ S ₂ /CoNiO _x nanorods with favorable stability at 1 A cm ^{â´2} for electrocatalytic water oxidation. Chemical Communications, 2019, 55, 1564-1567.	2.2	15
129	Improving energy transfer efficiency of dye-sensitized solar cell by fine tuning of dye planarity. Solar Energy, 2019, 187, 274-280.	2.9	24
130	Across the Board: Licheng Sun on the Mechanism of Oâ^'O Bond Formation in Photosystemâ€II. ChemSusChem, 2019, 12, 3401-3404.	3.6	9
131	Energy‣oss Reduction as a Strategy to Improve the Efficiency of Dye ensitized Solar Cells. Solar Rrl, 2019, 3, 1900253.	3.1	14
132	Boosting the power conversion efficiency of perovskite solar cells to 17.7% with an indolo[3,2- <i>b</i>]carbazole dopant-free hole transporting material by improving its spatial configuration. Journal of Materials Chemistry A, 2019, 7, 14835-14841.	5.2	39
133	Boosting nitrogen reduction reaction by bio-inspired FeMoS containing hybrid electrocatalyst over a wide pH range. Nano Energy, 2019, 62, 282-288.	8.2	108
134	Fine-tuning the coordination atoms of copper redox mediators: an effective strategy for boosting the photovoltage of dye-sensitized solar cells. Journal of Materials Chemistry A, 2019, 7, 12808-12814.	5.2	12
135	Paired Electrocatalytic Oxygenation and Hydrogenation of Organic Substrates with Water as the Oxygen and Hydrogen Source. Angewandte Chemie, 2019, 131, 9253-9257.	1.6	47
136	Paired Electrocatalytic Oxygenation and Hydrogenation of Organic Substrates with Water as the Oxygen and Hydrogen Source. Angewandte Chemie - International Edition, 2019, 58, 9155-9159.	7.2	188
137	Singlet Fission from Upper Excited Electronic States of Cofacial Perylene Dimer. Journal of Physical Chemistry Letters, 2019, 10, 2428-2433.	2.1	43
138	Artificial photosynthesis: opportunities and challenges of molecular catalysts. Chemical Society Reviews, 2019, 48, 2216-2264.	18.7	629
139	Ru-bda: Unique Molecular Water-Oxidation Catalysts with Distortion Induced Open Site and Negatively Charged Ligands. Journal of the American Chemical Society, 2019, 141, 5565-5580.	6.6	132
140	Two-dimensional Janus heterostructures for superior Z-scheme photocatalytic water splitting. Nano Energy, 2019, 59, 537-544.	8.2	121
141	13.6% Efficient Organic Dye-Sensitized Solar Cells by Minimizing Energy Losses of the Excited State. ACS Energy Letters, 2019, 4, 943-951.	8.8	284
142	Effects of ultrasonic waves on subcooled pool boiling on a small plain heating surface. Chemical Engineering Science, 2019, 201, 274-287.	1.9	21
143	Iron–Salen Complex and Co ²⁺ Ionâ€Derived Cobalt–Iron Hydroxide/Carbon Nanohybrid as an Efficient Oxygen Evolution Electrocatalyst. Advanced Science, 2019, 6, 1900117.	5.6	29
144	Surface-Supported Metal–Organic Framework Thin-Film-Derived Transparent CoS _{1.097} @N-Doped Carbon Film as an Efficient Counter Electrode for Bifacial Dye-Sensitized Solar Cells. ACS Applied Materials & Interfaces, 2019, 11, 14862-14870.	4.0	54

#	Article	IF	CITATIONS
145	Rational Design of Nanoarray Architectures for Electrocatalytic Water Splitting. Advanced Functional Materials, 2019, 29, 1808367.	7.8	298
146	Tailoring Active Sites in Mesoporous Defectâ€Rich NC/V _o â€WON Heterostructure Array for Superior Electrocatalytic Hydrogen Evolution. Advanced Energy Materials, 2019, 9, 1803693.	10.2	66
147	Optically Transparent Wood Substrate for Perovskite Solar Cells. ACS Sustainable Chemistry and Engineering, 2019, 7, 6061-6067.	3.2	89
148	Polymeric, Cost-Effective, Dopant-Free Hole Transport Materials for Efficient and Stable Perovskite Solar Cells. Journal of the American Chemical Society, 2019, 141, 19700-19707.	6.6	119
149	Dye-sensitized LaFeO ₃ photocathode for solar-driven H ₂ generation. Chemical Communications, 2019, 55, 12940-12943.	2.2	28
150	Iron carbonate hydroxide templated binary metal–organic frameworks for highly efficient electrochemical water oxidation. Chemical Communications, 2019, 55, 14773-14776.	2.2	41
151	Hollow Carbon@NiCo ₂ O ₄ Core–Shell Microspheres for Efficient Electrocatalytic Oxygen Evolution. Energy Technology, 2019, 7, 1800919.	1.8	5
152	Electrochemically polymerized poly (3, 4-phenylenedioxythiophene) as efficient and transparent counter electrode for dye sensitized solar cells. Electrochimica Acta, 2019, 300, 482-488.	2.6	38
153	Ironâ€Based Molecular Water Oxidation Catalysts: Abundant, Cheap, and Promising. Chemistry - an Asian Journal, 2019, 14, 31-43.	1.7	50
154	Molecular Engineering of Copper Phthalocyanines: A Strategy in Developing Dopantâ€Free Holeâ€Transporting Materials for Efficient and Ambientâ€Stable Perovskite Solar Cells. Advanced Energy Materials, 2019, 9, 1803287.	10.2	138
155	Composite Holeâ€Transport Materials Based on a Metalâ€Organic Copper Complex and Spiroâ€OMeTAD for Efficient Perovskite Solar Cells. Solar Rrl, 2018, 2, 1700073.	3.1	23
156	A Cu ₂ Se–Cu ₂ O film electrodeposited on titanium foil as a highly active and stable electrocatalyst for the oxygen evolution reaction. Chemical Communications, 2018, 54, 4979-4982.	2.2	42
157	Hierarchically Structured FeNiO _{<i>x</i>} H _{<i>y</i>} Electrocatalyst Formed by Inâ€Situ Transformation of Metal Phosphate for Efficient Oxygen Evolution Reaction. ChemSusChem, 2018, 11, 1761-1767.	3.6	20
158	Vertically Aligned Oxygenated-CoS ₂ –MoS ₂ Heteronanosheet Architecture from Polyoxometalate for Efficient and Stable Overall Water Splitting. ACS Catalysis, 2018, 8, 4612-4621.	5.5	290
159	Assembly of highly efficient photocatalytic CO2 conversion systems with ultrathin two-dimensional metal–organic framework nanosheets. Applied Catalysis B: Environmental, 2018, 227, 54-60.	10.8	140
160	Dendritic core-shell nickel-iron-copper metal/metal oxide electrode for efficient electrocatalytic water oxidation. Nature Communications, 2018, 9, 381.	5.8	322
161	Photon Up-Conversion via Epitaxial Surface-Supported Metal–Organic Framework Thin Films with Enhanced Photocurrent. ACS Applied Energy Materials, 2018, 1, 249-253.	2.5	36
162	Metal–organic frameworks (ZIF-67) as efficient cocatalysts for photocatalytic reduction of CO ₂ : the role of the morphology effect. Journal of Materials Chemistry A, 2018, 6, 4768-4775.	5.2	236

#	Article	IF	CITATIONS
163	Dye-Sensitized Photoelectrochemical Cells. , 2018, , 503-565.		3
164	DDQ as an effective p-type dopant for the hole-transport material X1 and its application in stable solid-state dye-sensitized solar cells. Journal of Energy Chemistry, 2018, 27, 413-418.	7.1	9
165	Highly efficient photocatalytic reduction of CO2 and H2O to CO and H2 with a cobalt bipyridyl complex. Journal of Energy Chemistry, 2018, 27, 502-506.	7.1	33
166	Integration of FeOOH and Zeolitic Imidazolate Frameworkâ€Derived Nanoporous Carbon as an Efficient Electrocatalyst for Water Oxidation. Advanced Energy Materials, 2018, 8, 1702598.	10.2	79
167	Atomically Thin Mesoporous In ₂ O _{3–} <i>_x</i> /In ₂ S ₃ Lateral Heterostructures Enabling Robust Broadbandâ€Light Photoâ€Electrochemical Water Splitting. Advanced Energy Materials. 2018. 8. 1701114.	10.2	106
168	Progress in hole-transporting materials for perovskite solar cells. Journal of Energy Chemistry, 2018, 27, 650-672.	7.1	90
169	Cu ₃ P/CuO Coreâ€Shell Nanorod Arrays as Highâ€Performance Electrocatalysts for Water Oxidation. ChemElectroChem, 2018, 5, 2064-2068.	1.7	20
170	Electronic and Structural Effects of Inner Sphere Coordination of Chloride to a Homoleptic Copper(II) Diimine Complex. Inorganic Chemistry, 2018, 57, 4556-4562.	1.9	31
171	Visible light-driven oxygen evolution using a binuclear Ru-bda catalyst. Chinese Journal of Catalysis, 2018, 39, 446-452.	6.9	10
172	Water Oxidation Initiated by In Situ Dimerization of the Molecular Ru(pdc) Catalyst. ACS Catalysis, 2018, 8, 4375-4382.	5.5	25
173	Experimental and Theoretical Investigation of the Function of 4- <i>tert</i> -Butyl Pyridine for Interface Energy Level Adjustment in Efficient Solid-State Dye-Sensitized Solar Cells. ACS Applied Materials & Interfaces, 2018, 10, 11572-11579.	4.0	15
174	Achieving High Openâ€Circuit Voltages up to 1.57 V in Holeâ€Transportâ€Materialâ€Free MAPbBr ₃ Solar Cells with Carbon Electrodes. Advanced Energy Materials, 2018, 8, 1701159.	10.2	55
175	Enhancing the Energyâ€Conversion Efficiency of Solidâ€State Dyeâ€Sensitized Solar Cells with a Chargeâ€Transfer Complex based on 2,3â€Dichloroâ€5,6â€dicyanoâ€1,4â€benzoquinone. Energy Technology, 20 752-758.)1188;6,	5
176	Promoting Active Sites in Core–Shell Nanowire Array as Mott–Schottky Electrocatalysts for Efficient and Stable Overall Water Splitting. Advanced Functional Materials, 2018, 28, 1704447.	7.8	225
177	Simultaneous oxidation of alcohols and hydrogen evolution in a hybrid system under visible light irradiation. Applied Catalysis B: Environmental, 2018, 225, 258-263.	10.8	71
178	Ultrafast Relaxation Dynamics in Zinc Tetraphenylporphyrin Surface-Mounted Metal Organic Framework. Journal of Physical Chemistry C, 2018, 122, 50-61.	1.5	48
179	Improved performance and air stability of perovskite solar cells based on low-cost organic hole-transporting material X60 by incorporating its dicationic salt. Science China Chemistry, 2018, 61, 172-179.	4.2	20
180	Inorganic Holeâ€Transporting Materials for Perovskite Solar Cells. Small Methods, 2018, 2, 1700280.	4.6	141

#	Article	IF	CITATIONS
181	Device Fabrication for Water Oxidation, Hydrogen Generation, and CO2 Reduction via Molecular Engineering. Joule, 2018, 2, 36-60.	11.7	98
182	Perovskite Hydroxide CoSn(OH) ₆ Nanocubes for Efficient Photoreduction of CO ₂ to CO. ACS Sustainable Chemistry and Engineering, 2018, 6, 781-786.	3.2	29
183	One plus one greater than two: high-performance inverted planar perovskite solar cells based on a composite Cul/CuSCN hole-transporting layer. Journal of Materials Chemistry A, 2018, 6, 21435-21444.	5.2	64
184	Direct Observation of Structural Evolution of Metal Chalcogenide in Electrocatalytic Water Oxidation. ACS Nano, 2018, 12, 12369-12379.	7.3	366
185	Metal–Organic Framework Thin Film-Based Dye Sensitized Solar Cells with Enhanced Photocurrent. Materials, 2018, 11, 1868.	1.3	19
186	Molecular Engineering of Dâ~'π–A Type of Blue-Colored Dyes for Highly Efficient Solid-State Dye-Sensitized Solar Cells through Co-Sensitization. ACS Applied Materials & Interfaces, 2018, 10, 35946-35952.	4.0	8
187	The Importance of Pendant Groups on Triphenylamineâ€Based Hole Transport Materials for Obtaining Perovskite Solar Cells with over 20% Efficiency. Advanced Energy Materials, 2018, 8, 1701209.	10.2	134
188	3D Core–Shell NiFeCr Catalyst on a Cu Nanoarray for Water Oxidation: Synergy between Structural and Electronic Modulation. ACS Energy Letters, 2018, 3, 2865-2874.	8.8	85
189	Molecular Engineering of Triphenylamine-Based Non-Fullerene Electron-Transport Materials for Efficient Rigid and Flexible Perovskite Solar Cells. ACS Applied Materials & Interfaces, 2018, 10, 38970-38977.	4.0	34
190	Enhanced S ₂ Fluorescence from a Free-Base Tetraphenylporphyrin Surface-Mounted Metal Organic Framework. Journal of Physical Chemistry C, 2018, 122, 23321-23328.	1.5	12
191	Chemical Dopant Engineering in Hole Transport Layers for Efficient Perovskite Solar Cells: Insight into the Interfacial Recombination. ACS Nano, 2018, 12, 10452-10462.	7.3	78
192	A facile route to grain morphology controllable perovskite thin films towards highly efficient perovskite solar cells. Nano Energy, 2018, 53, 405-414.	8.2	60
193	Model development and experimental verification for tubular solar still operating under vacuum condition. Energy, 2018, 157, 115-130.	4.5	44
194	Improving the performance of water splitting electrodes by composite plating with nano-SiO2. Electrochimica Acta, 2018, 281, 60-68.	2.6	6
195	D–A–D-Typed Hole Transport Materials for Efficient Perovskite Solar Cells: Tuning Photovoltaic Properties via the Acceptor Group. ACS Applied Materials & Interfaces, 2018, 10, 19697-19703.	4.0	101
196	Hierarchically Structured FeNiO x H y Electrocatalyst Formed by Inâ€Situ Transformation of Metal Phosphate for Efficient Oxygen Evolution Reaction. ChemSusChem, 2018, 11, 1740-1740.	3.6	0
197	Planar FAPbBr ₃ Solar Cells with Power Conversion Efficiency above 10%. ACS Energy Letters, 2018, 3, 1808-1814.	8.8	41
198	Improving the power conversion efficiency of solid state dye sensitized solar cells with a N-oxoammonium salt: 2,2,6,6-Tetramethyl-1-oxopiperidinebromide. Solar Energy, 2018, 170, 1001-1008.	2.9	4

#	Article	IF	CITATIONS
199	Molecular engineering of ionic type perylenediimide dimer-based electron transport materials for efficient planar perovskite solar cells. Materials Today Energy, 2018, 9, 264-270.	2.5	19
200	Orienting Active Crystal Planes of New Class Lacunaris Fe ₂ PO ₅ Polyhedrons for Robust Water Oxidation in Alkaline and Neutral Media. Advanced Functional Materials, 2018, 28, 1801397.	7.8	30
201	Electrical Behavior and Electron Transfer Modulation of Nickel–Copper Nanoalloys Confined in Nickel–Copper Nitrides Nanowires Array Encapsulated in Nitrogenâ€Doped Carbon Framework as Robust Bifunctional Electrocatalyst for Overall Water Splitting. Advanced Functional Materials, 2018, 28, 1803278.	7.8	84
202	Design and synthesis of dopant-free organic hole-transport materials for perovskite solar cells. Chemical Communications, 2018, 54, 9571-9574.	2.2	49
203	Efficient and Stable Dye-Sensitized Solar Cells Based on a Tetradentate Copper(II/I) Redox Mediator. ACS Applied Materials & Interfaces, 2018, 10, 30409-30416.	4.0	31
204	Why nature chose the Mn ₄ CaO ₅ cluster as water-splitting catalyst in photosystem II: a new hypothesis for the mechanism of O–O bond formation. Dalton Transactions, 2018, 47, 14381-14387.	1.6	77
205	Pushing the Envelope: Achieving an Openâ€Circuit Voltage of 1.18 V for Unalloyed MAPbl ₃ Perovskite Solar Cells of a Planar Architecture. Advanced Functional Materials, 2018, 28, 1801237.	7.8	26
206	Identifying MnVII-oxo Species during Electrochemical Water Oxidation by Manganese Oxide. IScience, 2018, 4, 144-152.	1.9	39
207	Highly Active Threeâ€Dimensional NiFe/Cu ₂ O Nanowires/Cu Foam Electrode for Water Oxidation. ChemSusChem, 2017, 10, 1475-1481.	3.6	53
208	Efficient dye-sensitized solar cells with [copper(6,6′-dimethyl-2,2′-bipyridine) ₂] ^{2+/1+} redox shuttle. RSC Advances, 2017, 7, 4611-4615.	, 1.7	48
209	Cu(II) Complexes as p-Type Dopants in Efficient Perovskite Solar Cells. ACS Energy Letters, 2017, 2, 497-503.	8.8	77
210	Molecular engineering of D–A–π–A sensitizers for highly efficient solid-state dye-sensitized solar cells. Journal of Materials Chemistry A, 2017, 5, 3157-3166.	5.2	41
211	Design, synthesis and application of a ï€-conjugated, non-spiro molecular alternative as hole-transport material for highly efficient dye-sensitized solar cells and perovskite solar cells. Journal of Power Sources, 2017, 344, 11-14.	4.0	49
212	A visualized study of the motion of individual bubbles in a venturi-type bubble generator. Progress in Nuclear Energy, 2017, 97, 74-89.	1.3	51
213	Photocatalytic H ₂ production using a hybrid assembly of an [FeFe]-hydrogenase model and CdSe quantum dot linked through a thiolato-functionalized cyclodextrin. Faraday Discussions, 2017, 198, 197-209.	1.6	27
214	Fabrication and Kinetic Study of a Ferrihydrite-Modified BiVO ₄ Photoanode. ACS Catalysis, 2017, 7, 1868-1874.	5.5	151
215	Incorporation of Counter Ions in Organic Molecules: New Strategy in Developing Dopantâ€Free Hole Transport Materials for Efficient Mixedâ€Ion Perovskite Solar Cells. Advanced Energy Materials, 2017, 7, 1602736.	10.2	72
216	Hollow Iron–Vanadium Composite Spheres: A Highly Efficient Ironâ€Based Water Oxidation Electrocatalyst without the Need for Nickel or Cobalt. Angewandte Chemie, 2017, 129, 3337-3341.	1.6	26

#	Article	IF	CITATIONS
217	Efficient perovskite solar cells employing a solution-processable copper phthalocyanine as a hole-transporting material. Science China Chemistry, 2017, 60, 423-430.	4.2	32
218	Rearranging from 6- to 7-coordination initiates the catalytic activity: An EPR study on a Ru-bda water oxidation catalyst. Coordination Chemistry Reviews, 2017, 346, 206-215.	9.5	34
219	Copper Oxide Film In-situ Electrodeposited from Cu(II) Complex as Highly Efficient Catalyst for Water Oxidation. Electrochimica Acta, 2017, 230, 501-507.	2.6	18
220	High-Performance Regular Perovskite Solar Cells Employing Low-Cost Poly(ethylenedioxythiophene) as a Hole-Transporting Material. Scientific Reports, 2017, 7, 42564.	1.6	52
221	Hollow Iron–Vanadium Composite Spheres: A Highly Efficient Ironâ€Based Water Oxidation Electrocatalyst without the Need for Nickel or Cobalt. Angewandte Chemie - International Edition, 2017, 56, 3289-3293.	7.2	216
222	Interfacial Engineering of Perovskite Solar Cells by Employing a Hydrophobic Copper Phthalocyanine Derivative as Holeâ€Transporting Material with Improved Performance and Stability. ChemSusChem, 2017, 10, 1838-1845.	3.6	54
223	Efficient Perovskite Solar Cells Based on a Solution Processable Nickel(II) Phthalocyanine and Vanadium Oxide Integrated Hole Transport Layer. Advanced Energy Materials, 2017, 7, 1602556.	10.2	107
224	Improvement of flow distribution and heat transfer performance of a self-similarity heat sink with a modification to its structure. Applied Thermal Engineering, 2017, 121, 163-171.	3.0	41
225	Tailor-Making Low-Cost Spiro[fluorene-9,9′-xanthene]-Based 3D Oligomers for Perovskite Solar Cells. CheM, 2017, 2, 676-687.	5.8	222
226	A Perylenediimide Tetramerâ€Based 3D Electron Transport Material for Efficient Planar Perovskite Solar Cell. Solar Rrl, 2017, 1, 1700046.	3.1	28
227	Novel and Stable D–Aâ~π–A Dyes for Efficient Solid-State Dye-Sensitized Solar Cells. ACS Omega, 2017, 2, 1812-1819.	1.6	19
228	In Situ Phaseâ€Induced Spatial Charge Separation in Core–Shell Oxynitride Nanocube Heterojunctions Realizing Robust Solar Water Splitting. Advanced Energy Materials, 2017, 7, 1700171.	10.2	39
229	Highly Efficient Photoelectrochemical Water Splitting with an Immobilized Molecular Co ₄ O ₄ Cubane Catalyst. Angewandte Chemie, 2017, 129, 7015-7019.	1.6	40
230	Highly Efficient Photoelectrochemical Water Splitting with an Immobilized Molecular Co ₄ O ₄ Cubane Catalyst. Angewandte Chemie - International Edition, 2017, 56, 6911-6915.	7.2	130
231	High performance solid-state dye-sensitized solar cells based on organic blue-colored dyes. Journal of Materials Chemistry A, 2017, 5, 1242-1247.	5.2	35
232	Inorganic Colloidal Perovskite Quantum Dots for Robust Solar CO ₂ Reduction. Chemistry - A European Journal, 2017, 23, 9481-9485.	1.7	225
233	Highly active and durable electrocatalytic water oxidation by a NiB0.45/NiO core-shell heterostructured nanoparticulate film. Nano Energy, 2017, 38, 175-184.	8.2	71
234	Biological approaches to artificial photosynthesis, fundamental processes and theoretical approaches: general discussion. Faraday Discussions, 2017, 198, 147-168.	1.6	0

#	Article	IF	CITATIONS
235	Inorganic assembly catalysts for artificial photosynthesis: general discussion. Faraday Discussions, 2017, 198, 481-507.	1.6	2
236	High-efficiency perovskite solar cells employing a conjugated donor–acceptor co-polymer as a hole-transporting material. RSC Advances, 2017, 7, 27189-27197.	1.7	27
237	Molecular catalysts for artificial photosynthesis: general discussion. Faraday Discussions, 2017, 198, 353-395.	1.6	6
238	Characteristics and mechanism of bubble breakup in a bubble generator developed for a small TMSR. Annals of Nuclear Energy, 2017, 109, 69-81.	0.9	41
239	Visible-light-absorbing semiconductor/molecular catalyst hybrid photoelectrodes for H ₂ or O ₂ evolution: recent advances and challenges. Sustainable Energy and Fuels, 2017, 1, 1641-1663.	2.5	68
240	Chemical and Physical Reduction of High Valence Ni States in Mesoporous NiO Film for Solar Cell Application. ACS Applied Materials & Interfaces, 2017, 9, 33470-33477.	4.0	58
241	Electrocatalytic water oxidation by copper(<scp>ii</scp>) complexes containing a tetra- or pentadentate amine-pyridine ligand. Chemical Communications, 2017, 53, 4374-4377.	2.2	71
242	Gas-templating of hierarchically structured Ni–Co–P for efficient electrocatalytic hydrogen evolution. Journal of Materials Chemistry A, 2017, 5, 7564-7570.	5.2	47
243	The Ru-tpc Water Oxidation Catalyst and Beyond: Water Nucleophilic Attack Pathway versus Radical Coupling Pathway. ACS Catalysis, 2017, 7, 2956-2966.	5.5	46
244	Simultaneously efficient light absorption and charge transport of phosphate and oxygen-vacancy confined in bismuth tungstate atomic layers triggering robust solar CO2 reduction. Nano Energy, 2017, 32, 359-366.	8.2	208
245	Re-Investigation of Cobalt Porphyrin for Electrochemical Water Oxidation on FTO Surface: Formation of CoOx as Active Species. ACS Catalysis, 2017, 7, 1143-1149.	5.5	74
246	Chemistry Future: Priorities and Opportunities from the Sustainability Perspective. ChemSusChem, 2017, 10, 6-13.	3.6	55
247	Water oxidation catalyzed by a charge-neutral mononuclear ruthenium(<scp>iii</scp>) complex. Dalton Transactions, 2017, 46, 1304-1310.	1.6	14
248	Stable and efficient PbS colloidal quantum dot solar cells incorporating low-temperature processed carbon paste counter electrodes. Solar Energy, 2017, 158, 28-33.	2.9	17
249	Active Sites Intercalated Ultrathin Carbon Sheath on Nanowire Arrays as Integrated Core–Shell Architecture: Highly Efficient and Durable Electrocatalysts for Overall Water Splitting. Small, 2017, 13, 1702018.	5.2	91
250	Ligandâ€Controlled Electrodeposition of Highly Intrinsically Active and Optically Transparent NiFeO _{<i>x</i>} H _{<i>y</i>} Film as a Water Oxidation Electrocatalyst. ChemSusChem, 2017, 10, 4690-4694.	3.6	7
251	Improvement of Electrochemical Water Oxidation by Fineâ€Tuning the Structure of Tetradentate N ₄ Ligands of Molecular Copper Catalysts. ChemSusChem, 2017, 10, 4581-4588.	3.6	38
252	Water Splitting via Decoupled Photocatalytic Water Oxidation and Electrochemical Proton Reduction Mediated by Electron oupledâ€Proton Buffer. Chemistry - an Asian Journal, 2017, 12, 2666-2669.	1.7	19

#	Article	IF	CITATIONS
253	Electrocatalytic Water Oxidation Promoted by 3 D Nanoarchitectured Turbostratic Î'â€MnO _{<i>x</i>} on Carbon Nanotubes. ChemSusChem, 2017, 10, 4472-4478.	3.6	18
254	Efficient and Stable Inverted Planar Perovskite Solar Cells Employing CuI as Holeâ€Transporting Layer Prepared by Solid–Gas Transformation. Energy Technology, 2017, 5, 1836-1843.	1.8	94
255	Defective and " <i>c</i> -Disordered― <i>Hortensia</i> -like Layered MnO _{<i>x</i>} as an Efficient Electrocatalyst for Water Oxidation at Neutral pH. ACS Catalysis, 2017, 7, 6311-6322.	5.5	62
256	Low-cost solution-processed digenite Cu ₉ S ₅ counter electrode for dye-sensitized solar cells. RSC Advances, 2017, 7, 38452-38457.	1.7	6
257	A solution-processable copper(<scp>ii</scp>) phthalocyanine derivative as a dopant-free hole-transporting material for efficient and stable carbon counter electrode-based perovskite solar cells. Journal of Materials Chemistry A, 2017, 5, 17862-17866.	5.2	67
258	Artificial Photosynthesis: Beyond Mimicking Nature. ChemSusChem, 2017, 10, 4228-4235.	3.6	59
259	Investigation on Formation Characteristics of Aerosol Particles during Wet Ammonia Desulfurization Process. Energy & Fuels, 2017, 31, 8374-8382.	2.5	12
260	Graphene Dots Embedded Phosphide Nanosheet-Assembled Tubular Arrays for Efficient and Stable Overall Water Splitting. ACS Applied Materials & Interfaces, 2017, 9, 24600-24607.	4.0	52
261	Temperature dependence of electrocatalytic water oxidation: a triple device model with a photothermal collector and photovoltaic cell coupled to an electrolyzer. Faraday Discussions, 2017, 198, 169-179.	1.6	32
262	An experimental study on Microbubble Emission Boiling in a subcooled pool: Heat transfer characteristics and visualized presentation. Experimental Thermal and Fluid Science, 2017, 80, 40-52.	1.5	17
263	Towards efficient and robust anodes for water splitting: Immobilization of Ru catalysts on carbon electrode and hematite by in situ polymerization. Catalysis Today, 2017, 290, 73-77.	2.2	22
264	Electrocatalytic water oxidation by a nickel oxide film derived from a molecular precursor. Chinese Journal of Catalysis, 2017, 38, 1812-1817.	6.9	7
265	Improving the Photocurrent in Quantum-Dot-Sensitized Solar Cells by Employing Alloy PbxCd1â^'xS Quantum Dots as Photosensitizers. Nanomaterials, 2016, 6, 97.	1.9	25
266	Efficient molecular ruthenium catalysts containing anionic ligands for water oxidation. Dalton Transactions, 2016, 45, 18459-18464.	1.6	12
267	Constructive Effects of Alkyl Chains: A Strategy to Design Simple and Non‣piro Hole Transporting Materials for High‣fficiency Mixedâ€Ion Perovskite Solar Cells. Advanced Energy Materials, 2016, 6, 1502536.	10.2	72
268	Promoting the Water Oxidation Catalysis by Synergistic Interactions between Ni(OH) ₂ and Carbon Nanotubes. Advanced Energy Materials, 2016, 6, 1600516.	10.2	68
269	Visible-light-driven selective oxidation of benzyl alcohol and thioanisole by molecular ruthenium catalyst modified hematite. Chemical Communications, 2016, 52, 9711-9714.	2.2	35
270	Visibleâ€Lightâ€Driven Water Oxidation on a Photoanode by Supramolecular Assembly of Photosensitizer and Catalyst. ChemPlusChem, 2016, 81, 1056-1059.	1.3	28

#	Article	IF	CITATIONS
271	Facile synthesized organic hole transporting material for perovskite solar cell with efficiency of 19.8%. Nano Energy, 2016, 23, 138-144.	8.2	253
272	Can aliphatic anchoring groups be utilised with dyes for p-type dye sensitized solar cells?. Dalton Transactions, 2016, 45, 7708-7719.	1.6	24
273	Facile synthesis of fluorene-based hole transport materials for highly efficient perovskite solar cells and solid-state dye-sensitized solar cells. Nano Energy, 2016, 26, 108-113.	8.2	103
274	Perovskite-based nanocubes with simultaneously improved visible-light absorption and charge separation enabling efficient photocatalytic CO2 reduction. Nano Energy, 2016, 30, 59-68.	8.2	92
275	Silicon Compound Decorated Photoanode for Performance Enhanced Visible Light Driven Water Splitting. Electrochimica Acta, 2016, 215, 682-688.	2.6	13
276	Catalytic Systems for Water Splitting. ChemPlusChem, 2016, 81, 1017-1019.	1.3	12
277	Towards a Bioinspiredâ€Systems Approach for Solar Fuel Devices. ChemPlusChem, 2016, 81, 1024-1027.	1.3	20
278	Carbon Nanotubes: Promoting the Water Oxidation Catalysis by Synergistic Interactions between Ni(OH)2and Carbon Nanotubes (Adv. Energy Mater. 15/2016). Advanced Energy Materials, 2016, 6, .	10.2	0
279	A Cobaltâ€Based Film for Highly Efficient Electrocatalytic Water Oxidation in Neutral Aqueous Solution. ChemCatChem, 2016, 8, 2757-2760.	1.8	13
280	Bis(1,1-bis(2-pyridyl)ethane)copper(<scp>i</scp> /i <scp>) as an efficient redox couple for liquid dye-sensitized solar cells. Journal of Materials Chemistry A, 2016, 4, 14550-14554.</scp>	5.2	63
281	Highly oriented MOF thin film-based electrocatalytic device for the reduction of CO ₂ to CO exhibiting high faradaic efficiency. Journal of Materials Chemistry A, 2016, 4, 15320-15326.	5.2	166
282	Molecular engineering for efficient and selective iron porphyrin catalysts for electrochemical reduction of CO ₂ to CO. Chemical Communications, 2016, 52, 14478-14481.	2.2	55
283	Conceptual design and experimental investigation involving a modular desalination system composed of arrayed tubular solar stills. Applied Energy, 2016, 179, 972-984.	5.1	52
284	Electrocatalytic water oxidation by a macrocyclic Cu(<scp>ii</scp>) complex in neutral phosphate buffer. Chemical Communications, 2016, 52, 10377-10380.	2.2	71
285	A new class of epitaxial porphyrin metal–organic framework thin films with extremely high photocarrier generation efficiency: promising materials for all-solid-state solar cells. Journal of Materials Chemistry A, 2016, 4, 12739-12747.	5.2	75
286	The Role of 3D Molecular Structural Control in New Hole Transport Materials Outperforming <i>Spiro</i> â€OMeTAD in Perovskite Solar Cells. Advanced Energy Materials, 2016, 6, 1601062.	10.2	87
287	Nickel–vanadium monolayer double hydroxide for efficient electrochemical water oxidation. Nature Communications, 2016, 7, 11981.	5.8	808
288	Highly Efficient Integrated Perovskite Solar Cells Containing a Small Molecule-PC ₇₀ BM Bulk Heterojunction Layer with an Extended Photovoltaic Response Up to 900 nm. Chemistry of Materials, 2016, 28, 8631-8639.	3.2	41

#	Article	IF	CITATIONS
289	Visible light-driven water oxidation with a subporphyrin sensitizer and a water oxidation catalyst. Chemical Communications, 2016, 52, 13702-13705.	2.2	61
290	Enhanced performance of perovskite solar cells with P3HT hole-transporting materials via molecular p-type doping. RSC Advances, 2016, 6, 108888-108895.	1.7	85
291	Effect of the S-to-S bridge on the redox properties and H ₂ activation performance of diiron complexes related to the [FeFe]-hydrogenase active site. Dalton Transactions, 2016, 45, 17687-17696.	1.6	19
292	Acceptor–Donor–Acceptor type ionic molecule materials for efficient perovskite solar cells and organic solar cells. Nano Energy, 2016, 30, 387-397.	8.2	79
293	Evident Enhancement of Photoelectrochemical Hydrogen Production by Electroless Deposition of M-B (M = Ni, Co) Catalysts on Silicon Nanowire Arrays. ACS Applied Materials & Interfaces, 2016, 8, 30143-30151.	4.0	40
294	A Cuâ€Based Nanoparticulate Film as Superâ€Active and Robust Catalyst Surpasses Pt for Electrochemical H ₂ Production from Neutral and Weak Acidic Aqueous Solutions. Advanced Energy Materials, 2016, 6, 1502319.	10.2	36
295	Enhanced Photocatalytic Hydrogen Production by Adsorption of an [FeFe]â€Hydrogenase Subunit Mimic on Selfâ€Assembled Membranes. European Journal of Inorganic Chemistry, 2016, 2016, 554-560.	1.0	26
296	Strategy to Boost the Efficiency of Mixed-Ion Perovskite Solar Cells: Changing Geometry of the Hole Transporting Material. ACS Nano, 2016, 10, 6816-6825.	7.3	127
297	Tailored design of ruthenium molecular catalysts with 2,2′-bypyridine-6,6′-dicarboxylate and pyrazole based ligands for water oxidation. Dalton Transactions, 2016, 45, 14689-14696.	1.6	17
298	Characterization of a trinuclear ruthenium species in catalytic water oxidation by Ru(bda)(pic) ₂ in neutral media. Chemical Communications, 2016, 52, 8619-8622.	2.2	36
299	A trinuclear ruthenium complex as a highly efficient molecular catalyst for water oxidation. Dalton Transactions, 2016, 45, 3814-3819.	1.6	22
300	A comprehensive comparison of dye-sensitized NiO photocathodes for solar energy conversion. Physical Chemistry Chemical Physics, 2016, 18, 10727-10738.	1.3	135
301	A nickel (II) PY5 complex as an electrocatalyst for water oxidation. Journal of Catalysis, 2016, 335, 72-78.	3.1	121
302	Photocatalytic water oxidation via combination of BiVO ₄ –RGO and molecular cobalt catalysts. Chemical Communications, 2016, 52, 3050-3053.	2.2	42
303	High conductivity Ag-based metal organic complexes as dopant-free hole-transport materials for perovskite solar cells with high fill factors. Chemical Science, 2016, 7, 2633-2638.	3.7	89
304	Application of benzodithiophene based A–D–A structured materials in efficient perovskite solar cells and organic solar cells. Nano Energy, 2016, 23, 40-49.	8.2	59
305	An iron-based thin film as a highly efficient catalyst for electrochemical water oxidation in a carbonate electrolyte. Chemical Communications, 2016, 52, 5753-5756.	2.2	51
306	A low-cost spiro[fluorene-9,9′-xanthene]-based hole transport material for highly efficient solid-state dye-sensitized solar cells and perovskite solar cells. Energy and Environmental Science, 2016, 9, 873-877.	15.6	362

#	Article	IF	CITATIONS
307	Electroless plated Ni–B films as highly active electrocatalysts for hydrogen production from water over a wide pH range. Nano Energy, 2016, 19, 98-107.	8.2	143
308	Stainless steel as an efficient electrocatalyst for water oxidation in alkaline solution. International Journal of Hydrogen Energy, 2016, 41, 5230-5233.	3.8	75
309	Boosting the efficiency and the stability of low cost perovskite solar cells by using CuPc nanorods as hole transport material and carbon as counter electrode. Nano Energy, 2016, 20, 108-116.	8.2	240
310	Visible light-driven water oxidation using a covalently-linked molecular catalyst–sensitizer dyad assembled on a TiO ₂ electrode. Chemical Science, 2016, 7, 1430-1439.	3.7	103
311	Effect of Bridgehead Steric Bulk on the Intramolecular C–H Heterolysis of [FeFe]-Hydrogenase Active Site Models Containing a P ₂ N ₂ Pendant Amine Ligand. Inorganic Chemistry, 2016, 55, 411-418.	1.9	17
312	Enhanced vapor bubble condensation and collapse with ultrasonic vibration. Experimental Thermal and Fluid Science, 2016, 70, 115-124.	1.5	34
313	EFFECTS OF A NONCONDENSABLE GAS ON THE MICROBUBBLE EMISSION BOILING. Heat Transfer Research, 2016, 47, 597-607.	0.9	0
314	Peripheral Hole Acceptor Moieties on an Organic Dye Improve Dye‧ensitized Solar Cell Performance. Advanced Science, 2015, 2, 1500174.	5.6	12
315	Assembling Supramolecular Dyeâ€6ensitized Photoelectrochemical Cells for Water Splitting. ChemSusChem, 2015, 8, 3992-3995.	3.6	24
316	Immobilization of a Molecular Ruthenium Catalyst on Hematite Nanorod Arrays for Water Oxidation with Stable Photocurrent. ChemSusChem, 2015, 8, 3242-3247.	3.6	49
317	Efficiency Enhanced Colloidal Mn-Doped Type II Core/Shell ZnSe/CdS Quantum Dot Sensitized Hybrid Solar Cells. Journal of Nanomaterials, 2015, 2015, 1-9.	1.5	11
318	High-efficiency dye-sensitized solar cells with molecular copper phenanthroline as solid hole conductor. Energy and Environmental Science, 2015, 8, 2634-2637.	15.6	149
319	Immobilizing Ru(bda) Catalyst on a Photoanode via Electrochemical Polymerization for Light-Driven Water Splitting. ACS Catalysis, 2015, 5, 3786-3790.	5.5	84
320	Alkene Epoxidation Catalysts [Ru(pdc)(tpy)] and [Ru(pdc)(pybox)] Revisited: Revealing a Unique Ru ^{IV} â•O Structure from a Dimethyl Sulfoxide Coordinating Complex. ACS Catalysis, 2015, 5, 3966-3972.	5.5	10
321	A study visualizing the collapse of vapor bubbles in a subcooled pool. International Journal of Heat and Mass Transfer, 2015, 88, 597-608.	2.5	57
322	Phenoxazineâ€Based Small Molecule Material for Efficient Perovskite Solar Cells and Bulk Heterojunction Organic Solar Cells. Advanced Energy Materials, 2015, 5, 1401720.	10.2	109
323	Design of a natural draft air-cooled condenser and its heat transfer characteristics in the passive residual heat removal system for 10ÂMW molten salt reactor experiment. Applied Thermal Engineering, 2015, 76, 423-434.	3.0	13
324	Integration of organometallic complexes with semiconductors and other nanomaterials for photocatalytic H2 production. Coordination Chemistry Reviews, 2015, 287, 1-14.	9.5	140

#	Article	IF	CITATIONS
325	A nonheme manganese(<scp>iv</scp>)–oxo species generated in photocatalytic reaction using water as an oxygen source. Chemical Communications, 2015, 51, 4013-4016.	2.2	30
326	Dipicolinic acid: a strong anchoring group with tunable redox and spectral behavior for stable dye-sensitized solar cells. Chemical Communications, 2015, 51, 3858-3861.	2.2	26
327	Phenoxazine-based panchromatic organic sensitizers for dye-sensitized solar cells. Dyes and Pigments, 2015, 116, 58-64.	2.0	21
328	1,1,2,2â€Tetrachloroethane (TeCA) as a Solvent Additive for Organic Hole Transport Materials and Its Application in Highly Efficient Solidâ€State Dyeâ€Sensitized Solar Cells. Advanced Energy Materials, 2015, 5, 1402340.	10.2	57
329	Sensitizer-Catalyst Assemblies for Water Oxidation. Inorganic Chemistry, 2015, 54, 2742-2751.	1.9	49
330	Novel Small Molecular Materials Based on Phenoxazine Core Unit for Efficient Bulk Heterojunction Organic Solar Cells and Perovskite Solar Cells. Chemistry of Materials, 2015, 27, 1808-1814.	3.2	100
331	Feature of acoustic sound signals involved in vapor bubble condensation and its application in identification of condensation regimes. Chemical Engineering Science, 2015, 137, 384-397.	1.9	21
332	Molecular complexes in water oxidation: Pre-catalysts or real catalysts. Journal of Photochemistry and Photobiology C: Photochemistry Reviews, 2015, 25, 71-89.	5.6	75
333	Organic Dye-Sensitized Tandem Photoelectrochemical Cell for Light Driven Total Water Splitting. Journal of the American Chemical Society, 2015, 137, 9153-9159.	6.6	327
334	Watching the dynamics of electrons and atoms at work in solar energy conversion. Faraday Discussions, 2015, 185, 51-68.	1.6	10
335	Highly Efficient Bioinspired Molecular Ru Water Oxidation Catalysts with Negatively Charged Backbone Ligands. Accounts of Chemical Research, 2015, 48, 2084-2096.	7.6	255
336	The mechanism of hydrogen evolution in Cu(bztpen)-catalysed water reduction: a DFT study. Dalton Transactions, 2015, 44, 9736-9739.	1.6	32
337	Recent Progress on Holeâ€Transporting Materials for Emerging Organometal Halide Perovskite Solar Cells. Advanced Energy Materials, 2015, 5, 1500213.	10.2	418
338	Electrochemical driven water oxidation by molecular catalysts in situ polymerized on the surface of graphite carbon electrode. Chemical Communications, 2015, 51, 7883-7886.	2.2	42
339	Photochemical hydrogen production from water catalyzed by CdTe quantum dots/molecular cobalt catalyst hybrid systems. Chemical Communications, 2015, 51, 7008-7011.	2.2	44
340	Evaluation of interfacial area transport equation in vertical bubbly two-phase flow in large diameter pipes. Annals of Nuclear Energy, 2015, 75, 199-209.	0.9	7
341	A closer mimic of the oxygen evolution complex of photosystem II. Science, 2015, 348, 635-636.	6.0	32
342	Visible Light-Driven Water Oxidation Promoted by Host–Guest Interaction between Photosensitizer and Catalyst with A High Quantum Efficiency. Journal of the American Chemical Society, 2015, 137, 4332-4335.	6.6	81

#	Article	IF	CITATIONS
343	In Situ Formation of Efficient Cobaltâ€Based Water Oxidation Catalysts from Co ²⁺ ontaining Tungstate and Molybdate Solutions. Chemistry - an Asian Journal, 2015, 10, 2228-2233.	1.7	12
344	A novel phenoxazine-based hole transport material for efficient perovskite solar cell. Journal of Energy Chemistry, 2015, 24, 698-706.	7.1	22
345	Engineering of hole-selective contact for low temperature-processed carbon counter electrode-based perovskite solar cells. Journal of Materials Chemistry A, 2015, 3, 24272-24280.	5.2	78
346	Slug flow in a vertical narrow rectangular channel – Laminar and turbulent regimes in the main flow and turbulent regime in the wake region of the Taylor bubble. Progress in Nuclear Energy, 2015, 85, 164-177.	1.3	6
347	Effect of liquid subcooling on acoustic characteristics during the condensation process of vapor bubbles in a subcooled pool. Nuclear Engineering and Design, 2015, 293, 492-502.	0.8	30
348	Construct Polyoxometalate Frameworks through Covalent Bonds. Inorganic Chemistry, 2015, 54, 8699-8704.	1.9	15
349	CdSe quantum dots/molecular cobalt catalyst co-grafted open porous NiO film as a photocathode for visible light driven H ₂ evolution from neutral water. Journal of Materials Chemistry A, 2015, 3, 18852-18859.	5.2	72
350	Crystal crosslinking. Nature Chemistry, 2015, 7, 684-685.	6.6	23
351	Efficient Electrocatalytic Water Oxidation by a Copper Oxide Thin Film in Borate Buffer. ACS Catalysis, 2015, 5, 627-630.	5.5	186
352	Across the Board: Licheng Sun. ChemSusChem, 2015, 8, 22-23.	3.6	2
353	The combination of a new organic D–π–A dye with different organic hole-transport materials for efficient solid-state dye-sensitized solar cells. Journal of Materials Chemistry A, 2015, 3, 4420-4427.	5.2	45
354	Recent advances in dye-sensitized photoelectrochemical cells for solar hydrogen production based on molecular components. Energy and Environmental Science, 2015, 8, 760-775.	15.6	363
355	Effects of noncondensable gas and ultrasonic vibration on vapor bubble condensing and collapsing. Experimental Thermal and Fluid Science, 2015, 61, 210-220.	1.5	27
356	Photocatalytic oxidation of organic compounds in a hybrid system composed of a molecular catalyst and visible light-absorbing semiconductor. Dalton Transactions, 2015, 44, 475-479.	1.6	22
357	Effects of rolling on resistance characteristics of single-phase flow in aÂ3Â×Â3 rod bundle. Progress in Nuclear Energy, 2015, 78, 231-239.	1.3	17
358	Novel organic dyes with anchoring group of quinoxaline-2, 3-diol and the application in dye-sensitized solar cells. Dyes and Pigments, 2015, 113, 581-587.	2.0	28
359	Model of bubble velocity vector measurement in upward and downward bubbly two-phase flows using a four-sensor optical probe. Progress in Nuclear Energy, 2015, 78, 110-120.	1.3	15
360	Integrated Design of Organic Hole Transport Materials for Efficient Solid‣tate Dye‣ensitized Solar Cells. Advanced Energy Materials, 2015, 5, 1401185.	10.2	59

#	Article	IF	CITATIONS
361	EFFECT OF THE CHROMOPHORES STRUCTURES ON THE PERFORMANCE OF SOLID-STATE DYE SENSITIZED SOLAR CELLS. Nano, 2014, 09, 1440005.	0.5	7
362	Solar cells and photocatalytic systems: general discussion. Faraday Discussions, 2014, 176, 313-331.	1.6	1
363	Catalytic water oxidation based on Ag(<scp>i</scp>)-substituted Keggin polyoxotungstophosphate. Dalton Transactions, 2014, 43, 17406-17415.	1.6	17
364	Experimental Study on Resistance Characteristics in a 3 $ ilde{A}$ — 3 Rod Bundle. , 2014, , .		0
365	Photocatalytic Water Oxidation by Molecular Assemblies Based on Cobalt Catalysts. ChemSusChem, 2014, 7, 2453-2456.	3.6	43
366	Experimental and theoretical analysis of bubble rising velocity in a 3×3 rolling rod bundle under stagnant condition. Annals of Nuclear Energy, 2014, 72, 471-481.	0.9	13
367	Nickel Complex with Internal Bases as Efficient Molecular Catalyst for Photochemical H ₂ Production. ChemSusChem, 2014, 7, 2889-2897.	3.6	18
368	Water Oxidation. European Journal of Inorganic Chemistry, 2014, 2014, 571-572.	1.0	3
369	Artificial photosynthesis: photosensitizer/catalyst supramolecular assemblies for light driven water oxidation. Faraday Discussions, 2014, 176, 225-232.	1.6	18
370	Experimental study and numerical optimization on a vane-type separator for bubble separation in TMSR. Progress in Nuclear Energy, 2014, 74, 1-13.	1.3	62
371	Slug behavior and pressure drop of adiabatic slug flow in a narrow rectangular duct under inclined conditions. Annals of Nuclear Energy, 2014, 64, 21-31.	0.9	12
372	Air–water two-phase flow in a rolling 3×3 rod bundle under stagnant condition. Experimental Thermal and Fluid Science, 2014, 55, 200-209.	1.5	7
373	Effects of void fraction correlations on pressure gradient separation ofÂair–water two-phase flow in vertical mini rectangular ducts. Progress in Nuclear Energy, 2014, 70, 84-90.	1.3	23
374	Local interfacial parameter distribution for two-phase flow under rolling conditions using a four-sensor optical probe. Annals of Nuclear Energy, 2014, 66, 124-132.	0.9	16
375	Influence of different methylene units on the performance of rhodanine organic dyes for dye-sensitized solar cells. RSC Advances, 2014, 4, 4811.	1.7	5
376	Characteristics of slug flow in a vertical narrow rectangular channel. Experimental Thermal and Fluid Science, 2014, 53, 1-16.	1.5	30
377	A super-efficient cobalt catalyst for electrochemical hydrogen production from neutral water with 80 mV overpotential. Energy and Environmental Science, 2014, 7, 329-334.	15.6	121
378	Water Oxidation Catalyzed by Mononuclear Ruthenium Complexes with a 2,2′-Bipyridine-6,6′-dicarboxylate (bda) Ligand: How Ligand Environment Influences the Catalytic Behavior. Inorganic Chemistry, 2014, 53, 1307-1319.	1.9	61

#	Article	IF	CITATIONS
379	Photoisomerization of the cyanoacrylic acid acceptor group – a potential problem for organic dyes in solar cells. Physical Chemistry Chemical Physics, 2014, 16, 2251.	1.3	53
380	A Molecular Copper Catalyst for Electrochemical Water Reduction with a Large Hydrogenâ€Generation Rate Constant in Aqueous Solution. Angewandte Chemie - International Edition, 2014, 53, 13803-13807.	7.2	166
381	Highly efficient and robust molecular water oxidation catalysts based on ruthenium complexes. Chemical Communications, 2014, 50, 12947-12950.	2.2	144
382	A visualized study of micro-bubble emission boiling. International Communications in Heat and Mass Transfer, 2014, 59, 148-157.	2.9	6
383	Artificial photosynthesis: A two-electrode photoelectrochemical cell for light driven water oxidation with molecular components. Electrochimica Acta, 2014, 149, 337-340.	2.6	11
384	Improved Performance of Colloidal CdSe Quantum Dot-Sensitized Solar Cells by Hybrid Passivation. ACS Applied Materials & Interfaces, 2014, 6, 18808-18815.	4.0	36
385	Two Redox Couples are Better Than One: Improved Current and Fill Factor from Cobaltâ€Based Electrolytes in Dye ensitized Solar Cells. Advanced Energy Materials, 2014, 4, 1301273.	10.2	17
386	The influence of a S-to-S bridge in diiron dithiolate models on the oxidation reaction: a mimic of the Hairox state of [FeFe]-hydrogenases. Chemical Communications, 2014, 50, 9255-9258.	2.2	15
387	Photocatalytic water oxidation at soft interfaces. Chemical Science, 2014, 5, 2683-2687.	3.7	62
388	Simultaneous Multiple Wavelength Upconversion in a Core–Shell Nanoparticle for Enhanced Near Infrared Light Harvesting in a Dye-Sensitized Solar Cell. ACS Applied Materials & Interfaces, 2014, 6, 18018-18025.	4.0	77
389	Triphenylamine Groups Improve Blocking Behavior of Phenoxazine Dyes in Cobaltâ€Electrolyteâ€Based Dyeâ€ S ensitized Solar Cells. ChemPhysChem, 2014, 15, 3476-3483.	1.0	17
390	An organic hydrophilic dye for water-based dye-sensitized solar cells. Physical Chemistry Chemical Physics, 2014, 16, 19964-19971.	1.3	43
391	Highly efficient molecular nickel catalysts for electrochemical hydrogen production from neutral water. Chemical Communications, 2014, 50, 14153-14156.	2.2	65
392	Molecular engineering of small molecules donor materials based on phenoxazine core unit for solution-processed organic solar cells. Journal of Materials Chemistry A, 2014, 2, 10465-10469.	5.2	15
393	Phenothiazine derivatives-based D–π–A and D–A–π–A organic dyes for dye-sensitized solar cells. RSC Advances, 2014, 4, 24377.	1.7	38
394	Artificial photosynthesis – functional devices for light driven water splitting with photoactive anodes based on molecular catalysts. Physical Chemistry Chemical Physics, 2014, 16, 12008.	1.3	84
395	Pt-free tandem molecular photoelectrochemical cells for water splitting driven by visible light. Physical Chemistry Chemical Physics, 2014, 16, 25234-25240.	1.3	135
396	Visible Light-Driven Water Splitting in Photoelectrochemical Cells with Supramolecular Catalysts on Photoanodes. ACS Catalysis, 2014, 4, 2347-2350.	5.5	115

#	Article	IF	CITATIONS
397	Effect of Different Numbers of â^'CH ₂ – Units on the Performance of Isoquinolinium Dyes. ACS Applied Materials & Interfaces, 2014, 6, 3907-3914.	4.0	11
398	Organic D–π–A sensitizer with pyridinium as the acceptor group for dye-sensitized solar cells. RSC Advances, 2014, 4, 34644-34648.	1.7	7
399	Redox Reactions of [FeFe]-Hydrogenase Models Containing an Internal Amine and a Pendant Phosphine. Inorganic Chemistry, 2014, 53, 1555-1561.	1.9	24
400	Research on frictional resistance of bubbly flow in rolling rectangular ducts. Nuclear Engineering and Design, 2014, 278, 108-116.	0.8	5
401	Immobilization of a molecular catalyst on carbon nanotubes for highly efficient electro-catalytic water oxidation. Chemical Communications, 2014, 50, 13948-13951.	2.2	42
402	Red-Absorbing Cationic Acceptor Dyes for Photocathodes in Tandem Solar Cells. Journal of Physical Chemistry C, 2014, 118, 16536-16546.	1.5	51
403	Poly(3,4-ethylenedioxythiophene) Hole-Transporting Material Generated by Photoelectrochemical Polymerization in Aqueous and Organic Medium for All-Solid-State Dye-Sensitized Solar Cells. Journal of Physical Chemistry C, 2014, 118, 16591-16601.	1.5	48
404	Efficient Organic Sensitizers with Pyridineâ€ <i>N</i> â€oxide as an Anchor Group for Dye‧ensitized Solar Cells. ChemSusChem, 2014, 7, 2640-2646.	3.6	14
405	Highâ€Performance Photoelectrochemical Cells Based on a Binuclear Ruthenium Catalyst for Visibleâ€Lightâ€Driven Water Oxidation. ChemSusChem, 2014, 7, 2801-2804.	3.6	79
406	Carbazoleâ€Based Holeâ€Transport Materials for Efficient Solidâ€State Dyeâ€Sensitized Solar Cells and Perovskite Solar Cells. Advanced Materials, 2014, 26, 6629-6634.	11.1	369
407	Comparison of local interfacial characteristics between vertical upward and downward two-phase flows using a four-sensor optical probe. International Journal of Heat and Mass Transfer, 2014, 77, 1183-1196.	2.5	17
408	Hydrodynamics of slug flow in a vertical narrow rectangular channel under laminar flow condition. Annals of Nuclear Energy, 2014, 73, 465-477.	0.9	2
409	Electrochemical and Photoelectrochemical Water Oxidation by Supported Cobalt–Oxo Cubanes. ACS Catalysis, 2014, 4, 804-809.	5.5	73
410	Structure Engineering of Hole–Conductor Free Perovskite-Based Solar Cells with Low-Temperature-Processed Commercial Carbon Paste As Cathode. ACS Applied Materials & Interfaces, 2014, 6, 16140-16146.	4.0	245
411	Homogeneous Oxidation of Water by Iron Complexes with Macrocyclic Ligands. Chemistry - an Asian Journal, 2014, 9, 1515-1518.	1.7	42
412	AgTFSI as pâ€Type Dopant for Efficient and Stable Solidâ€State Dyeâ€Sensitized and Perovskite Solar Cells. ChemSusChem, 2014, 7, 3252-3256.	3.6	114
413	Application of Small Molecule Donor Materials Based on Phenothiazine Core Unit in Bulk Heterojunction Solar Cells. Journal of Physical Chemistry C, 2014, 118, 16851-16855.	1.5	24
414	Intramolecular Iron-Mediated C–H Bond Heterolysis with an Assist of Pendant Base in a [FeFe]-Hydrogenase Model. Journal of the American Chemical Society, 2014, 136, 16817-16823.	6.6	38

#	Article	IF	CITATIONS
415	Conceptual design and analysis of a passive residual heat removal system for a 10ÂMW molten salt reactor experiment. Progress in Nuclear Energy, 2014, 70, 149-158.	1.3	20
416	Synthesis, electrochemistry and photo-induced electron transfer of unsymmetrical dinuclear ruthenium osmium 2,2′-bipyridine complexes. Journal of Photochemistry and Photobiology A: Chemistry, 2014, 287, 40-48.	2.0	2
417	Effect of rolling motion on transient flow resistance of two-phase flow in a narrow rectangular duct. Annals of Nuclear Energy, 2014, 64, 135-143.	0.9	22
418	Void fraction of dispersed bubbly flow in a narrow rectangular channel under rolling conditions. Progress in Nuclear Energy, 2014, 70, 256-265.	1.3	17
419	Flow fluctuation behaviors of single-phase forced circulation under rolling conditions. Ocean Engineering, 2014, 82, 115-122.	1.9	18
420	Investigation of the interfacial parameter distribution in a bubbly flow in a narrow rectangular channel under inclined and rolling conditions. Progress in Nuclear Energy, 2014, 73, 64-74.	1.3	12
421	Evaluation analysis of correlations for predicting the void fraction and slug velocity of slug flow in an inclined narrow rectangular duct. Nuclear Engineering and Design, 2014, 273, 155-164.	0.8	5
422	Characteristics of slug flow in a narrow rectangular channel under inclined conditions. Progress in Nuclear Energy, 2014, 76, 24-35.	1.3	6
423	Enhancement of p-Type Dye-Sensitized Solar Cell Performance by Supramolecular Assembly of Electron Donor and Acceptor. Scientific Reports, 2014, 4, 4282.	1.6	59
424	Two-Phase Slug Flow in a Narrow Rectangular Channel Under Inclined Conditions. , 2014, , .		0
425	Reactions of [FeFe]-hydrogenase models involving the formation of hydrides related to proton reduction and hydrogen oxidation. Dalton Transactions, 2013, 42, 12059.	1.6	104
426	Highly efficient organic dyes containing a benzopyran ring as a π–bridge for DSSCs. RSC Advances, 2013, 3, 12688.	1.7	5
427	Visible light-driven water oxidation catalyzed by mononuclear ruthenium complexes. Journal of Catalysis, 2013, 306, 129-132.	3.1	58
428	A theoretical analysis about the effect of aspect ratio on single-phase laminar flow in rectangular ducts. Progress in Nuclear Energy, 2013, 65, 1-7.	1.3	19
429	Experimental study of interfacial parameter distributions in upward bubbly flow under vertical and inclined conditions. Experimental Thermal and Fluid Science, 2013, 47, 117-125.	1.5	16
430	Efficient p-type dye-sensitized solar cells based on disulfide/thiolate electrolytes. Nanoscale, 2013, 5, 7963.	2.8	50
431	Effect of the acceptor on the performance of dye-sensitized solar cells. Physical Chemistry Chemical Physics, 2013, 15, 17452.	1.3	37
432	Catalytic Activation of H ₂ under Mild Conditions by an [FeFe]-Hydrogenase Model via an Active μ-Hydride Species. Journal of the American Chemical Society, 2013, 135, 13688-13691.	6.6	107

#	Article	IF	CITATIONS
433	Electrocatalytic hydrogen evolution from neutral water by molecular cobalt tripyridine–diamine complexes. Chemical Communications, 2013, 49, 9455.	2.2	91
434	Convergent/Divergent Synthesis of a Linkerâ€Varied Series of Dyes for Dye‧ensitized Solar Cells Based on the D35 Donor. Advanced Energy Materials, 2013, 3, 1647-1656.	10.2	103
435	Dye-sensitized solar cells based on hydroquinone/benzoquinone as bio-inspired redox couple with different counter electrodes. Physical Chemistry Chemical Physics, 2013, 15, 15146.	1.3	19
436	Frictional resistance of adiabatic two-phase flow in narrow rectangular duct under rolling conditions. Annals of Nuclear Energy, 2013, 53, 109-119.	0.9	25
437	An experimental study of bubble sliding characteristics in narrow channel. International Journal of Heat and Mass Transfer, 2013, 57, 89-99.	2.5	43
438	Linker Unit Modification of Triphenylamine-Based Organic Dyes for Efficient Cobalt Mediated Dye-Sensitized Solar Cells. Journal of Physical Chemistry C, 2013, 117, 21029-21036.	1.5	79
439	A new type of organic sensitizers with pyridine-N-oxide as the anchoring group for dye-sensitized solar cells. RSC Advances, 2013, 3, 13677.	1.7	35
440	Efficient solid state dye-sensitized solar cells based on an oligomer hole transport material and an organic dye. Journal of Materials Chemistry A, 2013, 1, 14467.	5.2	67
441	Efficient Panchromatic Organic Sensitizers with Dihydrothiazole Derivative as π-Bridge for Dye-Sensitized Solar Cells. ACS Applied Materials & Interfaces, 2013, 5, 10960-10965.	4.0	35
442	Axial anchoring designed silicon–porphyrin sensitizers for efficient dye-sensitized solar cells. Chemical Communications, 2013, 49, 11785.	2.2	26
443	Efficient Organic Dyeâ€5ensitized Solar Cells: Molecular Engineering of Donor–Acceptor–Acceptor cationic dyes. ChemSusChem, 2013, 6, 2322-2329.	3.6	26
444	Chemical and photocatalytic water oxidation by mononuclear Ru catalysts. Chinese Journal of Catalysis, 2013, 34, 1489-1495.	6.9	39
445	Tuning band structures of dyes for dye-sensitized solar cells: effect of different π-bridges on the performance of cells. RSC Advances, 2013, 3, 15734.	1.7	23
446	Tetranuclear Iron Complexes Bearing Benzenetetrathiolate Bridges as Four-Electron Transformation Templates and Their Electrocatalytic Properties for Proton Reduction. Inorganic Chemistry, 2013, 52, 1798-1806.	1.9	31
447	Highly efficient iso-quinoline cationic organic dyes without vinyl groups for dye-sensitized solar cells. Journal of Materials Chemistry A, 2013, 1, 2441.	5.2	30
448	Promoting the Activity of Catalysts for the Oxidation of Water with Bridged Dinuclear Ruthenium Complexes. Angewandte Chemie - International Edition, 2013, 52, 3398-3401.	7.2	110
449	Coâ€sensitization of Organic Dyes for Efficient Dyeâ€Sensitized Solar Cells. ChemSusChem, 2013, 6, 70-77.	3.6	56
450	Microbubble emission boiling in scbcooled pool boiling and the role of Marangoni convection in its formation. Experimental Thermal and Fluid Science, 2013, 50, 97-106.	1.5	27

#	Article	IF	CITATIONS
451	Effect of rolling motion on single-phase laminar flow resistance of forced circulation with different pump head. Annals of Nuclear Energy, 2013, 54, 141-148.	0.9	31
452	Visible Light Driven Water Splitting in a Molecular Device with Unprecedentedly High Photocurrent Density. Journal of the American Chemical Society, 2013, 135, 4219-4222.	6.6	330
453	Tuning the HOMO and LUMO Energy Levels of Organic Dyes with <i>N</i> -Carboxomethylpyridinium as Acceptor To Optimize the Efficiency of Dye-Sensitized Solar Cells. Journal of Physical Chemistry C, 2013, 117, 9076-9083.	1.5	72
454	New Organic Dyes with a Phenanthrenequinone Derivative as the ï€-Conjugated Bridge for Dye-Sensitized Solar Cells. Journal of Physical Chemistry C, 2013, 117, 12936-12941.	1.5	29
455	Initial Light Soaking Treatment Enables Hole Transport Material to Outperform Spiro-OMeTAD in Solid-State Dye-Sensitized Solar Cells. Journal of the American Chemical Society, 2013, 135, 7378-7385.	6.6	138
456	Molecular Design and Performance of Hydroxylpyridium Sensitizers for Dye-Sensitized Solar Cells. ACS Applied Materials & Interfaces, 2013, 5, 5227-5231.	4.0	50
457	Catalytic Water Oxidation by Mononuclear Ru Complexes with an Anionic Ancillary Ligand. Inorganic Chemistry, 2013, 52, 2505-2518.	1.9	77
458	Dye-Sensitized Photoelectrochemical Cells. , 2013, , 385-441.		2
459	Enhanced Performance of pâ€Type Dyeâ€5ensitized Solar Cells Based on Ultrasmall Mgâ€Doped CuCrO ₂ Nanocrystals. ChemSusChem, 2013, 6, 1432-1437.	3.6	68
460	Degradation of Cyanoacrylic Acidâ€Based Organic Sensitizers in Dyeâ€5ensitized Solar Cells. ChemSusChem, 2013, 6, 1270-1275.	3.6	56
461	Insights into Ru-Based Molecular Water Oxidation Catalysts: Electronic and Noncovalent-Interaction Effects on Their Catalytic Activities. Inorganic Chemistry, 2013, 52, 7844-7852.	1.9	136
462	Study on the Characteristics in the Liquid Slug of Rising Slug Flow in Narrow Rectangular Channel. , 2013, , .		0
463	Experimental Study of a Gas Separator for MSR Gas Removal System. , 2013, , .		3
464	Research on transient flow resistance of two-phase in narrow rectangular channel under rolling motions. , 2013, , .		2
465	Effect of rolling motion on local characteristics of gas-liquid two-phase flow using an optical probe. , 2013, , .		0
466	Experimental investigations of single-phase and two-phase flow resistance in narrow rectangular duct under rolling condition. , 2013, , .		1
467	An experimental research on microbubble emission boiling. , 2013, , .		0
468	Characteristics of slug flow in narrow rectangular channels under vertical condition. , 2013, , .		0

#	Article	IF	CITATIONS
469	Flow regimes of adiabatic gas-liquid two-phase under rolling conditions. , 2013, , .		Ο
470	Experimental Investigation on Bubbly Flow in Rectangular Channel Under Rolling Condition. , 2013, , .		0
471	2-(5-Bromothiophen-2-yl)-5-[5-(10-ethylphenothiazin-3-yl)thiophen-2-yl]-1,3,4-oxadiazole. Acta Crystallographica Section E: Structure Reports Online, 2012, 68, o1383-o1384.	0.2	0
472	10-Ethyl-3-(5-methyl-1,3,4-oxadiazol-2-yl)-10H-phenothiazine. Acta Crystallographica Section E: Structure Reports Online, 2012, 68, o649-o649.	0.2	2
473	Development of an organic redox couple and organic dyes for aqueous dye-sensitized solar cells. Energy and Environmental Science, 2012, 5, 9752.	15.6	55
474	Solvent-free ionic liquid electrolytes without elemental iodine for dye-sensitized solar cells. Physical Chemistry Chemical Physics, 2012, 14, 11592.	1.3	28
475	Dyeâ€Sensitized Solar Cells Based on a Donor–Acceptor System with a Pyridine Cation as an Electronâ€Withdrawing Anchoring Group. Chemistry - A European Journal, 2012, 18, 16196-16202.	1.7	57
476	Molecular Design of Dâ€Ï€â€A Type II Organic Sensitizers for Dye Sensitized Solar Cells. Chinese Journal of Chemistry, 2012, 30, 2315-2321.	2.6	14
477	Simple Nickelâ€Based Catalyst Systems Combined With Graphitic Carbon Nitride for Stable Photocatalytic Hydrogen Production in Water. ChemSusChem, 2012, 5, 2133-2138.	3.6	126
478	Highly efficient and robust molecular ruthenium catalysts for water oxidation. Proceedings of the National Academy of Sciences of the United States of America, 2012, 109, 15584-15588.	3.3	202
479	A highly efficient colourless sulfur/iodide-based hybrid electrolyte for dye-sensitized solar cells. RSC Advances, 2012, 2, 3625.	1.7	39
480	Pendant amine bases speed up proton transfers to metals by splitting the barriers. Chemical Communications, 2012, 48, 4450.	2.2	30
481	Femtosecond to millisecond studies of electron transfer processes in a donor–(π-spacer)–acceptor series of organic dyes for solar cells interacting with titania nanoparticles and ordered nanotube array films. Physical Chemistry Chemical Physics, 2012, 14, 2816.	1.3	40
482	Water Oxidation Catalysis: Influence of Anionic Ligands upon the Redox Properties and Catalytic Performance of Mononuclear Ruthenium Complexes. Inorganic Chemistry, 2012, 51, 3388-3398.	1.9	77
483	Effect of Electrolyte Composition on Electron Injection and Dye Regeneration Dynamics in Complete Organic Dye Sensitized Solar Cells Probed by Time-Resolved Laser Spectroscopy. Journal of Physical Chemistry C, 2012, 116, 26227-26238.	1.5	25
484	Iodine/iodide-free redox shuttles for liquid electrolyte-based dye-sensitized solar cells. Energy and Environmental Science, 2012, 5, 9180.	15.6	146
485	Oxygen evolution at functionalized carbon surfaces: a strategy for immobilization of molecular water oxidation catalysts. Chemical Communications, 2012, 48, 10025.	2.2	61
486	Recent progress in electrochemical hydrogen production with earth-abundant metal complexes as catalysts. Energy and Environmental Science, 2012, 5, 6763.	15.6	474

#	Article	IF	CITATIONS
487	Phenoxazine dyes in solid-state dye-sensitized solar cells. Journal of Photochemistry and Photobiology A: Chemistry, 2012, 239, 55-59.	2.0	10
488	Efficient Dye‣ensitized Solar Cells Based on Hydroquinone/Benzoquinone as a Bioinspired Redox Couple. Angewandte Chemie - International Edition, 2012, 51, 9896-9899.	7.2	61
489	Multielectronâ€Transfer Templates via Consecutive Twoâ€Electron Transformations: Iron–Sulfur Complexes Relevant to Biological Enzymes. Chemistry - A European Journal, 2012, 18, 13968-13973.	1.7	31
490	Photocatalytic H2 production in aqueous solution with host-guest inclusions formed by insertion of an FeFe-hydrogenase mimic and an organic dye into cyclodextrins. Energy and Environmental Science, 2012, 5, 8220.	15.6	114
491	Oxygen evolution from water oxidation on molecular catalysts confined in the nanocages of mesoporous silicas. Energy and Environmental Science, 2012, 5, 8229.	15.6	58
492	Use of colloidal upconversion nanocrystals for energy relay solar cell light harvesting in the near-infrared region. Journal of Materials Chemistry, 2012, 22, 16709.	6.7	101
493	Dye-Sensitized Photoelectrochemical Cells. , 2012, , 479-542.		17
494	Combining a Small Hole-Conductor Molecule for Efficient Dye Regeneration and a Hole-Conducting Polymer in a Solid-State Dye-Sensitized Solar Cell. Journal of Physical Chemistry C, 2012, 116, 18070-18078.	1.5	36
495	Synthesis and ECL performance of highly efficient bimetallic ruthenium tris-bipyridyl complexes. Dalton Transactions, 2012, 41, 12434.	1.6	16
496	Toward Controlling Water Oxidation Catalysis: Tunable Activity of Ruthenium Complexes with Axial Imidazole/DMSO Ligands. Journal of the American Chemical Society, 2012, 134, 18868-18880.	6.6	101
497	Photo-induced electron transfer study of D-ï€-A sensitizers with different type of anchoring groups for dye-sensitized solar cells. RSC Advances, 2012, 2, 6011.	1.7	8
498	Ru complexes containing pyridine dicarboxylate ligands: electronic effects on their catalytic activity toward wateroxidation. Faraday Discussions, 2012, 155, 267-275.	1.6	34
499	Tetrathiafulvalene as a one-electron iodine-free organic redox mediator in electrolytes for dye-sensitized solar cells. RSC Advances, 2012, 2, 1083-1087.	1.7	24
500	Nitro group as a new anchoring group for organic dyes in dye-sensitized solar cells. Chemical Communications, 2012, 48, 6663.	2.2	65
501	Phosphine Coordination to a Cobalt Diimine–Dioxime Catalyst Increases Stability during Light-Driven H ₂ Production. Inorganic Chemistry, 2012, 51, 2115-2120.	1.9	98
502	Electrochemical water oxidation by photo-deposited cobalt-based catalyst on a nano-structured TiO2 electrode. Science China Chemistry, 2012, 55, 1976-1981.	4.2	5
503	Comparing spiro-OMeTAD and P3HT hole conductors in efficient solid state dye-sensitized solar cells. Physical Chemistry Chemical Physics, 2012, 14, 779-789.	1.3	118
504	Type-II colloidal quantum dot sensitized solar cells with a thiourea based organic redox couple. Journal of Materials Chemistry, 2012, 22, 6032.	6.7	41

#	Article	IF	CITATIONS
505	Efficient dye-sensitized solar cells based on an iodine-free electrolyte using l-cysteine/l-cystine as a redox couple. Energy and Environmental Science, 2012, 5, 6290-6293.	15.6	56
506	A molecular ruthenium catalyst with water-oxidation activity comparable to that of photosystem II. Nature Chemistry, 2012, 4, 418-423.	6.6	1,131
507	Photocatalytic Water Reduction and Study of the Formation of Fe ^I Fe ^O Species in Diiron Catalyst Sytems. ChemSusChem, 2012, 5, 913-919.	3.6	42
508	Visible light driven hydrogen production from a photo-active cathode based on a molecular catalyst and organic dye-sensitized p-type nanostructured NiO. Chemical Communications, 2012, 48, 988-990.	2.2	237
509	Photochemical hydrogen production with molecular devices comprising a zinc porphyrin and a cobaloxime catalyst. Science China Chemistry, 2012, 55, 1274-1282.	4.2	16
510	Polymerization of rac-lactide catalyzed by group 4 metal complexes containing chiral N atoms. Polymer Bulletin, 2012, 68, 1789-1799.	1.7	6
511	Effects of rolling on characteristics of single-phase water flow in narrow rectangular ducts. Nuclear Engineering and Design, 2012, 247, 221-229.	0.8	51
512	Engineering of highly efficient tetrahydroquinoline sensitizers for dye-sensitized solar cells. Tetrahedron, 2012, 68, 552-558.	1.0	42
513	Novel D–π–A type II organic sensitizers for dye sensitized solar cells. Tetrahedron Letters, 2012, 53, 3425-3428.	0.7	21
514	Towards A Solar Fuel Device: Lightâ€Driven Water Oxidation Catalyzed by a Supramolecular Assembly. Angewandte Chemie - International Edition, 2012, 51, 2417-2420.	7.2	126
515	Ce ^{IV} ―and Lightâ€Driven Water Oxidation by [Ru(terpy)(pic) ₃] ²⁺ Analogues: Catalytic and Mechanistic Studies. ChemSusChem, 2011, 4, 238-244.	3.6	72
516	Chemical and photochemical oxidation of organic substrates by ruthenium aqua complexes with water as an oxygen source. Chemical Communications, 2011, 47, 8949.	2.2	45
517	A thiolate/disulfide ionic liquid electrolyte for organic dye-sensitized solar cells based on Pt-free counter electrodes. Chemical Communications, 2011, 47, 10124.	2.2	54
518	Efficient organic dye sensitized solar cells based on modified sulfide/polysulfide electrolyte. Journal of Materials Chemistry, 2011, 21, 5573.	6.7	32
519	Modifying organic phenoxazine dyes for efficient dye-sensitized solar cells. Journal of Materials Chemistry, 2011, 21, 12462.	6.7	79
520	A photo-induced electron transfer study of an organic dye anchored on the surfaces of TiO2 nanotubes and nanoparticles. Physical Chemistry Chemical Physics, 2011, 13, 4032.	1.3	45
521	Mapping the frontier electronic structures of triphenylamine based organic dyes at TiO ₂ interfaces. Physical Chemistry Chemical Physics, 2011, 13, 3534-3546.	1.3	10
522	Ruthenium sensitizer with a thienylvinylbipyridyl ligand for dye-sensitized solar cells. Dalton Transactions, 2011, 40, 8361.	1.6	10

#	Article	IF	CITATIONS
523	Highly Efficient CdS Quantum Dot-Sensitized Solar Cells Based on a Modified Polysulfide Electrolyte. Journal of the American Chemical Society, 2011, 133, 8458-8460.	6.6	257
524	Solid state dye-sensitized solar cells prepared by infiltrating a molten hole conductor into a mesoporous film at a temperature below 150°C. Synthetic Metals, 2011, 161, 2280-2283.	2.1	6
525	Organic Redox Couples and Organic Counter Electrode for Efficient Organic Dye-Sensitized Solar Cells. Journal of the American Chemical Society, 2011, 133, 9413-9422.	6.6	227
526	Solar cells sensitized with type-II ZnSe–CdS core/shell colloidal quantum dots. Chemical Communications, 2011, 47, 1536-1538.	2.2	161
527	Visible light-driven water oxidation—from molecular catalysts to photoelectrochemical cells. Energy and Environmental Science, 2011, 4, 3296.	15.6	209
528	Iodine-free redox couples for dye-sensitized solar cells. Journal of Materials Chemistry, 2011, 21, 10592.	6.7	137
529	Promoting Effect of Electrostatic Interaction between a Cobalt Catalyst and a Xanthene Dye on Visible-Light-Driven Electron Transfer and Hydrogen Production. Journal of Physical Chemistry C, 2011, 115, 15089-15096.	1.5	73
530	Approaches to efficient molecular catalyst systems for photochemical H2 production using [FeFe]-hydrogenase active site mimics. Dalton Transactions, 2011, 40, 12793.	1.6	116
531	Highly Efficient Solidâ€State Dyeâ€Sensitized Solar Cells Based on Triphenylamine Dyes. Advanced Functional Materials, 2011, 21, 2944-2952.	7.8	178
532	Synthesis of a [3Fe2S] Cluster with Low Redox Potential from [2Fe2S] Hydrogenase Models: Electrochemical and Photochemical Generation of Hydrogen. European Journal of Inorganic Chemistry, 2011, 2011, 1100-1105.	1.0	19
533	A Doubleâ€Band Tandem Organic Dyeâ€sensitized Solar Cell with an Efficiency of 11.5 %. ChemSusChem, 2011, 4, 609-612.	3.6	33
534	Molecular Design to Improve the Performance of Donor–π Acceptor Nearâ€IR Organic Dye‧ensitized Solar Cells. ChemSusChem, 2011, 4, 1601-1605.	3.6	30
535	Quantum Rodâ€Sensitized Solar Cells. ChemSusChem, 2011, 4, 1741-1744.	3.6	10
536	Structural Modifications of Mononuclear Ruthenium Complexes:†A Combined Experimental and Theoretical Study on the Kinetics of Rutheniumâ€Catalyzed Water Oxidation. Angewandte Chemie - International Edition, 2011, 50, 445-449.	7.2	177
537	Highly Efficient Oxidation of Water by a Molecular Catalyst Immobilized on Carbon Nanotubes. Angewandte Chemie - International Edition, 2011, 50, 12276-12279.	7.2	193
538	Asymmetric oxidation of sulfides with H2O2 catalyzed by titanium complexes of Schiff bases bearing a dicumenyl salicylidenyl unit. Applied Organometallic Chemistry, 2011, 25, 325-330.	1.7	22
539	A Suzukiâ€type crossâ€coupling reaction of arylacetylene halides with arylboronic acids. Applied Organometallic Chemistry, 2011, 25, 514-520.	1.7	9
540	Isolated Supramolecular [Ru(bpy) ₃]–Viologen–[Ru(bpy) ₃] Complexes with Trapped CB[7,8] and Photoinduced Electronâ€Transfer Study in Nonaqueous Solution. Chemistry - A European Journal, 2011, 17, 11604-11612.	1.7	15

#	Article	IF	CITATIONS
541	Pure Organic Redox Couple for Quantumâ€Dotâ€Sensitized Solar Cells. Chemistry - A European Journal, 2011, 17, 6330-6333.	1.7	16
542	Phenoxazine Dyes for Dye‣ensitized Solar Cells: Relationship Between Molecular Structure and Electron Lifetime. Chemistry - A European Journal, 2011, 17, 6415-6424.	1.7	107
543	Synthesis and Catalytic Water Oxidation Activities of Ruthenium Complexes Containing Neutral Ligands. Chemistry - A European Journal, 2011, 17, 9520-9528.	1.7	33
544	The OO Bonding in Water Oxidation: the Electronic Structure Portrayal of a Concerted Oxygen Atom–Proton Transfer Pathway. Chemistry - A European Journal, 2011, 17, 8313-8317.	1.7	40
545	Stable dye-sensitized solar cells based on organic chromophores and ionic liquid electrolyte. Solar Energy, 2011, 85, 1189-1194.	2.9	36
546	Synthesis of New Chiral Schiff Bases Containing Bromo- and Iodo-Functionalized Hydroxynaphthalene Frameworks. Synthetic Communications, 2011, 41, 1381-1393.	1.1	3
547	Research and Development of Dye-Sensitized Solar Cells in the Center for Molecular Devices: From Molecules to Modules. , 2011, , .		1
548	Design of Organic Dyes and Cobalt Polypyridine Redox Mediators for High-Efficiency Dye-Sensitized Solar Cells. Journal of the American Chemical Society, 2010, 132, 16714-16724.	6.6	1,000
549	Homogeneous photocatalytic production of hydrogen from water by a bioinspired [Fe ₂ S ₂] catalyst with high turnover numbers. Dalton Transactions, 2010, 39, 1204-1206.	1.6	143
550	Photochemical H2 production with noble-metal-free molecular devices comprising a porphyrin photosensitizer and a cobaloxime catalyst. Chemical Communications, 2010, 46, 8806.	2.2	160
551	Dye-Sensitized Solar Cells. Chemical Reviews, 2010, 110, 6595-6663.	23.0	8,072
552	A photoelectrochemical device for visible light driven water splitting by a molecular ruthenium catalyst assembled on dye-sensitized nanostructured TiO2. Chemical Communications, 2010, 46, 7307.	2.2	232
553	Highly enantioselective sulfoxidation with vanadium catalysts of Schiff bases derived from bromo- and iodo-functionalized hydroxynaphthaldehydes. Journal of Catalysis, 2010, 273, 177-181.	3.1	39
554	Hydrogen Production by Nobleâ€Metalâ€Free Molecular Catalysts and Related Nanomaterials. ChemSusChem, 2010, 3, 551-554.	3.6	75
555	Double‣ayered NiO Photocathodes for pâ€Type DSSCs with Record IPCE. Advanced Materials, 2010, 22, 1759-1762.	11.1	303
556	Attachment of a Hydrogenâ€Bonding Carboxylate Side Chain to an [FeFe]â€Hydrogenase Model Complex: Influence on the Catalytic Mechanism. Chemistry - A European Journal, 2010, 16, 2537-2546.	1.7	46
557	Chemical and Photochemical Water Oxidation Catalyzed by Mononuclear Ruthenium Complexes with a Negatively Charged Tridentate Ligand. Chemistry - A European Journal, 2010, 16, 4659-4668.	1.7	154
558	Tuning the HOMO Energy Levels of Organic Dyes for Dye ensitized Solar Cells Based on Br ^{â~'} /Br ₃ ^{â~'} Electrolytes. Chemistry - A European Journal, 2010, 16, 13127-13138.	1.7	112

#	Article	IF	CITATIONS
559	Evolution of O ₂ in a Sevenâ€Coordinate Ru ^{IV} Dimer Complex with a [HOHOH] ^{â^²} Bridge: A Computational Study. Angewandte Chemie - International Edition, 2010, 49, 1773-1777.	7.2	155
560	Efficient Organicâ€Dye‧ensitized Solar Cells Based on an Iodineâ€Free Electrolyte. Angewandte Chemie - International Edition, 2010, 49, 7328-7331.	7.2	112
561	Chemical and Lightâ€Driven Oxidation of Water Catalyzed by an Efficient Dinuclear Ruthenium Complex. Angewandte Chemie - International Edition, 2010, 49, 8934-8937.	7.2	199
562	A new class of organic dyes based on acenaphthopyrazine for dye-sensitized solar cells. Journal of Photochemistry and Photobiology A: Chemistry, 2010, 213, 152-157.	2.0	10
563	Formation of a new hybrid complex via coordination interaction between 5,10,15-tritolyl-20-(4- and) Tj ETQq1 1 (polyoxometalate (M=Co2+ and Ni2+). Inorganica Chimica Acta, 2010, 363, 2185-2192.	0.784314 1.2	rgBT /Overlo 42
564	PdCl2-catalyzed cross-coupling reaction of arylacetylene iodides with arylboronic acids to diarylacetylenes. Tetrahedron Letters, 2010, 51, 3626-3628.	0.7	19
565	Effect of different electron donating groups on the performance of dye-sensitized solar cells. Dyes and Pigments, 2010, 84, 62-68.	2.0	132
566	Preparation and structure of an enantiomeric water-bridged dinuclear indium complex containing two homochiral N atoms and its performance as an initiator in polymerization of rac-lactide. Inorganic Chemistry Communication, 2010, 13, 968-971.	1.8	32
567	Parallel onnected monolithic dyeâ€sensitised solar modules. Progress in Photovoltaics: Research and Applications, 2010, 18, 340-345.	4.4	35
568	Visible Light-Driven Water Oxidation by a Molecular Ruthenium Catalyst in Homogeneous System. Inorganic Chemistry, 2010, 49, 209-215.	1.9	244
569	Synthesis and Mechanistic Studies of Organic Chromophores with Different Energy Levels for p-Type Dye-Sensitized Solar Cells. Journal of Physical Chemistry C, 2010, 114, 4738-4748.	1.5	174
570	Photocatalytic Hydrogen Production from Water by Noble-Metal-Free Molecular Catalyst Systems Containing Rose Bengal and the Cobaloximes of BF _{<i>x</i>} -Bridged Oxime Ligands. Journal of Physical Chemistry C, 2010, 114, 15868-15874.	1.5	151
571	Wave-Function Engineering of CdSe/CdS Core/Shell Quantum Dots for Enhanced Electron Transfer to a TiO ₂ Substrate. Journal of Physical Chemistry C, 2010, 114, 15184-15189.	1.5	60
572	Surface Molecular Quantification and Photoelectrochemical Characterization of Mixed Organic Dye and Coadsorbent Layers on TiO ₂ for Dye-Sensitized Solar Cells. Journal of Physical Chemistry C, 2010, 114, 11903-11910.	1.5	59
573	Influence of Triple Bonds as π-Spacer Units in Metal-Free Organic Dyes for Dye-Sensitized Solar Cells. Journal of Physical Chemistry C, 2010, 114, 11305-11313.	1.5	134
574	How the Nature of Triphenylamine-Polyene Dyes in Dye-Sensitized Solar Cells Affects the Open-Circuit Voltage and Electron Lifetimes. Langmuir, 2010, 26, 2592-2598.	1.6	359
575	Molecular Design of Anthracene-Bridged Metal-Free Organic Dyes for Efficient Dye-Sensitized Solar Cells. Journal of Physical Chemistry C, 2010, 114, 9101-9110.	1.5	216
576	ECL performance of ruthenium tris-bipyridyl complexes covalently linked with phenothiazine through different bridge. Dalton Transactions, 2010, 39, 8626.	1.6	26

#	Article	IF	CITATIONS
577	Structural Modification of Organic Dyes for Efficient Coadsorbent-Free Dye-Sensitized Solar Cells. Journal of Physical Chemistry C, 2010, 114, 2799-2805.	1.5	120
578	Synthesis of Tri- and Disalicylaldehydes and Their Chiral Schiff Base Compounds. Synthetic Communications, 2010, 40, 1074-1081.	1.1	10
579	Distance and Driving Force Dependencies of Electron Injection and Recombination Dynamics in Organic Dye-Sensitized Solar Cellsâ€. Journal of Physical Chemistry B, 2010, 114, 14358-14363.	1.2	63
580	Visible light-driven water oxidation catalyzed by a highly efficient dinuclear ruthenium complex. Chemical Communications, 2010, 46, 6506.	2.2	115
581	Electronic and molecular structures of organic dye/TiO2 interfaces for solar cell applications: a core level photoelectron spectroscopy study. Physical Chemistry Chemical Physics, 2010, 12, 1507.	1.3	56
582	Synthesis and DNA photocleavage study of Ru(bpy)32+-(CH2)n-MV2+ complexes. Dalton Transactions, 2010, 39, 4411.	1.6	15
583	Unusual partner radical trimer formation in a host complex of cucurbit[8]uril, ruthenium(ii) tris-bipyridine linked phenol and methyl viologen. Chemical Communications, 2010, 46, 463-465.	2.2	20
584	Preparation and structures of enantiomeric dinuclear zirconium and hafnium complexes containing two homochiral N atoms, and their catalytic property for polymerization of rac-lactide. Dalton Transactions, 2010, 39, 4440.	1.6	39
585	Interrogating the ultrafast dynamics of an efficient dye for sunlight conversion. Physical Chemistry Chemical Physics, 2010, 12, 8098.	1.3	22
586	A Lightâ€Resistant Organic Sensitizer for Solarâ€Cell Applications. Angewandte Chemie - International Edition, 2009, 48, 1576-1580.	7.2	223
587	Intra- and intermolecular interaction ECL study of novel ruthenium tris-bipyridyl complexes with different amine reductants. Dalton Transactions, 2009, , 7969.	1.6	31
588	The Effect of UV-Irradiation (under Short-Circuit Condition) on Dye-Sensitized Solar Cells Sensitized with a Ru-Complex Dye Functionalized with a (diphenylamino)Styryl-Thiophen Group. International Journal of Photoenergy, 2009, 2009, 1-9.	1.4	4
589	High Incident Photonâ€toâ€Current Conversion Efficiency of pâ€Type Dyeâ€Sensitized Solar Cells Based on NiO and Organic Chromophores. Advanced Materials, 2009, 21, 2993-2996.	11.1	173
590	Selective Positioning of CB[8] on Two Linked Viologens and Electrochemically Driven Movement of the Host Molecule. European Journal of Organic Chemistry, 2009, 2009, 1163-1172.	1.2	23
591	An evaluation of prediction methods for saturated flow boiling heat transfer in mini-channels. International Journal of Heat and Mass Transfer, 2009, 52, 5323-5329.	2.5	187
592	Electrogenerated chemiluminescence of benzo 15â€crownâ€5 derivatives. Journal of Physical Organic Chemistry, 2009, 22, 1-8.	0.9	8
593	Evaluation analysis of prediction methods for two-phase flow pressure drop in mini-channels. International Journal of Multiphase Flow, 2009, 35, 47-54.	1.6	265
594	Synthesis, protonation and electrochemical properties of trinuclear NiFe2 complexes Fe2(CO)6(1¼3-S)2[Ni(Ph2PCH2)2NR] (R=n-Bu, Ph) with an internal pendant nitrogen base as a proton relay. Inorganica Chimica Acta, 2009, 362, 372-376.	1.2	14

#	Article	IF	CITATIONS
595	Protophilicity, electrochemical property, and desulfurization of diiron dithiolate complexes containing a functionalized C2 bridge with two vicinal basic sites. Polyhedron, 2009, 28, 1138-1144.	1.0	8
596	Synthesis and characterization of carboxy-functionalized diiron model complexes of [FeFe]-hydrogenases: Decarboxylation of Ph2PCH2COOH promoted by a diiron azadithiolate complex. Journal of Organometallic Chemistry, 2009, 694, 2309-2314.	0.8	25
597	Photochemical hydrogen production catalyzed by polypyridyl ruthenium–cobaloxime heterobinuclear complexes with different bridges. Journal of Organometallic Chemistry, 2009, 694, 2814-2819.	0.8	116
598	Light-driven hydrogen production catalysed by transition metal complexes in homogeneous systems. Dalton Transactions, 2009, , 6458.	1.6	241
599	Visible light driven H2 production in molecular systems employing colloidal MoS2 nanoparticles as catalyst. Chemical Communications, 2009, , 4536.	2.2	116
600	Preparation, Facile Deprotonation, and Rapid H/D Exchange of the μ-Hydride Diiron Model Complexes of the [FeFe]-Hydrogenase Containing a Pendant Amine in a Chelating Diphosphine Ligand. Inorganic Chemistry, 2009, 48, 11551-11558.	1.9	84
601	Effect on Cell Efficiency following Thermal Degradation of Dye-Sensitized Mesoporous Electrodes Using N719 and D5 Sensitizers. Journal of Physical Chemistry C, 2009, 113, 18902-18906.	1.5	20
602	Experimental Study on the Fluid Stratification Mechanism in the Density Lock. Journal of Nuclear Science and Technology, 2009, 46, 925-932.	0.7	1
603	Study of Highly Efficient Bimetallic Ruthenium Tris-bipyridyl ECL Labels for Coreactant System. Analytical Chemistry, 2009, 81, 10227-10231.	3.2	49
604	Isolated Seven-Coordinate Ru(IV) Dimer Complex with [HOHOH] ^{â^'} Bridging Ligand as an Intermediate for Catalytic Water Oxidation. Journal of the American Chemical Society, 2009, 131, 10397-10399.	6.6	461
605	Rhodaninedyes for dye-sensitized solar cells :  spectroscopy, energy levels and photovoltaic performance. Physical Chemistry Chemical Physics, 2009, 11, 133-141.	1.3	178
606	Tuning of phenoxazine chromophores for efficient organic dye-sensitized solar cells. Chemical Communications, 2009, , 6288.	2.2	156
607	Symmetric and unsymmetric donor functionalization. comparing structural and spectral benefits of chromophores for dye-sensitized solar cells. Journal of Materials Chemistry, 2009, 19, 7232.	6.7	177
608	Nucleophilic Attack of Hydroxide on a Mn ^V Oxo Complex: A Model of the Oâ^'O Bond Formation in the Oxygen Evolving Complex of Photosystem II. Journal of the American Chemical Society, 2009, 131, 8726-8727.	6.6	238
609	A New Dinuclear Ruthenium Complex as an Efficient Water Oxidation Catalyst. Inorganic Chemistry, 2009, 48, 2717-2719.	1.9	143
610	Efficient near infrared D–π–A sensitizers with lateral anchoring group for dye-sensitized solar cells. Chemical Communications, 2009, , 4031.	2.2	112
611	Two Novel Carbazole Dyes for Dye-Sensitized Solar Cells with Open-Circuit Voltages up to 1 V Based on Br ^{â^'} /Br ₃ ^{â^'} Electrolytes. Organic Letters, 2009, 11, 5542-5545.	2.4	166
612	Highly Efficient Organic Sensitizers for Solid-State Dye-Sensitized Solar Cells. Journal of Physical Chemistry C, 2009, 113, 16816-16820.	1.5	91

#	Article	IF	CITATIONS
613	Effect of Anchoring Group on Electron Injection and Recombination Dynamics in Organic Dye-Sensitized Solar Cells. Journal of Physical Chemistry C, 2009, 113, 3881-3886.	1.5	185
614	A metal-free "black dye―for panchromatic dye-sensitized solar cells. Energy and Environmental Science, 2009, 2, 674.	15.6	153
615	Structures, protonation, and electrochemical properties of diiron dithiolate complexes containing pyridyl-phosphine ligands. Dalton Transactions, 2009, , 1919.	1.6	61
616	Redox-induced partner radical formation and its dynamic balance with radical dimer in cucurbit[8]uril. Physical Chemistry Chemical Physics, 2009, 11, 11134.	1.3	28
617	Asymmetric oxidation of sulfides with hydrogen peroxide catalyzed by a vanadium complex of a new chiral NOO-ligand. Catalysis Communications, 2009, 11, 294-297.	1.6	23
618	Light driven formation of a supramolecular system with three CB[8]s locked between redox-active Ru(bpy)3 complexes. Organic and Biomolecular Chemistry, 2009, 7, 3605.	1.5	16
619	A comparative study of a polyene-diphenylaniline dye and Ru(dcbpy)2(NCS)2 in electrolyte-based and solid-state dye-sensitized solar cells. Thin Solid Films, 2008, 516, 7214-7217.	0.8	18
620	Photoinduced Intramolecular Charge Transfer and S ₂ Fluorescence in Thiophene‥€â€Conjugated Donor–Acceptor Systems: Experimental and TDDFT Studies. Chemistry - A European Journal, 2008, 14, 6935-6947.	1.7	203
621	Influence of substituents in the salicylaldehydeâ€derived Schiff bases on vanadiumâ€catalyzed asymmetric oxidation of sulfides. Applied Organometallic Chemistry, 2008, 22, 253-257.	1.7	24
622	Synthesis and structure of a µâ€oxo diiron(III) complex with an <i>N</i> â€pyridylmethylâ€ <i>N</i> , <i>N</i> â€bis(4â€methylbenzimidazolâ€2â€yl)amine ligand and its catalytic property for hydrocarbon oxidation. Applied Organometallic Chemistry, 2008, 22, 573-576.	1.7	7
623	Asymmetric epoxidation of chromenes catalyzed by chiral pyrrolidine SalenMn(III) complexes with an an anchored functional group. Applied Organometallic Chemistry, 2008, 22, 592-597.	1.7	2
624	A Triphenylamine Dye Model for the Study of Intramolecular Energy Transfer and Charge Transfer in Dye‧ensitized Solar Cells. Advanced Functional Materials, 2008, 18, 3461-3468.	7.8	131
625	Synthesis and characterization of some new mononuclear ruthenium complexes containing 4-(un)substituted dipyridylpyrazole ligands. Polyhedron, 2008, 27, 1168-1176.	1.0	11
626	Oligothiophene-2-yl-vinyl bridged mono- and binuclear ruthenium(II) tris-bipyridine complexes: Synthesis, photophysics, electrochemistry and electrogenerated chemiluminescence. Journal of Organometallic Chemistry, 2008, 693, 46-56.	0.8	21
627	A new square planar mononuclear MnIII complex for catalytic epoxidation of stilbene. Journal of Organometallic Chemistry, 2008, 693, 1150-1153.	0.8	7
628	Pendant bases as proton transfer relays in diiron dithiolate complexes inspired by [Fe–Fe] hydrogenase active site. Journal of Organometallic Chemistry, 2008, 693, 2828-2834.	0.8	46
629	[FeFe]-Hydrogenase active site models with relatively low reduction potentials: Diiron dithiolate complexes containing rigid bridges. Journal of Inorganic Biochemistry, 2008, 102, 952-959.	1.5	16
630	An azadithiolate bridged Fe2S2 complex as active site model of FeFe-hydrogenase covalently linked to a Re(CO)3(bpy)(py) photosensitizer aiming for light-driven hydrogen production. Comptes Rendus Chimie, 2008, 11, 915-921.	0.2	30

#	Article	IF	CITATIONS
631	Intramolecularly two-centered cooperation catalysis for the synthesis of cyclic carbonates from CO2 and epoxides. Tetrahedron Letters, 2008, 49, 6589-6592.	0.7	89
632	Photoinduced intramolecular charge-transfer state in thiophene-π-conjugated donor–acceptor molecules. Journal of Molecular Structure, 2008, 876, 102-109.	1.8	72
633	Diiron dithiolate complexes containing intra-ligand NHâ√S hydrogen bonds: [FeFe] hydrogenase active site models for the electrochemical proton reduction of HOAc with low overpotential. Dalton Transactions, 2008, , 2400.	1.6	37
634	A Host-Induced Intramolecular Charge-Transfer Complex and Light-Driven Radical Cation Formation of a Molecular Triad with Cucurbit[8]uril. Journal of Organic Chemistry, 2008, 73, 3775-3783.	1.7	59
635	Design of an Organic Chromophore for P-Type Dye-Sensitized Solar Cells. Journal of the American Chemical Society, 2008, 130, 8570-8571.	6.6	371
636	Molecular Engineering of Organic Sensitizers for Dye-Sensitized Solar Cell Applications. Journal of the American Chemical Society, 2008, 130, 6259-6266.	6.6	625
637	Effect of Different Dye Baths and Dye-Structures on the Performance of Dye-Sensitized Solar Cells Based on Triphenylamine Dyes. Journal of Physical Chemistry C, 2008, 112, 11023-11033.	1.5	432
638	Noncovalent Assembly of a Metalloporphyrin and an Iron Hydrogenase Active-Site Model: Photo-Induced Electron Transfer and Hydrogen Generation. Journal of Physical Chemistry B, 2008, 112, 8198-8202.	1.2	150
639	A proton–hydride diiron complex with a base-containing diphosphine ligand relevant to the [FeFe]-hydrogenase active site. Chemical Communications, 2008, , 5800.	2.2	73
640	Supramolecular self-assembly of a [2Fe2S] complex with a hydrophilic phosphine ligand. CrystEngComm, 2008, 10, 267-269.	1.3	18
641	CO-Migration in the Ligand Substitution Process of the Chelating Diphosphite Diiron Complex (μ-pdt)[Fe(CO) ₃][Fe(CO){(EtO) ₂ PN(Me)P(OEt) ₂ }]. Inorganic Chemistry, 2008, 47, 6948-6955.	1.9	50
642	Preparation, characterization and electrochemistry of an iron-only hydrogenase active site model covalently linked to a ruthenium tris(bipyridine) photosensitizer. Journal of Coordination Chemistry, 2008, 61, 1856-1861.	0.8	17
643	Visible Light-Driven Electron Transfer and Hydrogen Generation Catalyzed by Bioinspired [2Fe2S] Complexes. Inorganic Chemistry, 2008, 47, 2805-2810.	1.9	203
644	Association of ruthenium complexes [Ru(bpy)3]2+ or [Ru(bpy)2(Mebpy-py)]2+ with Dawson polyanions α-[P2W18O62]6– or α2-[FellI(H2O)P2W17O61]7–. Canadian Journal of Chemistry, 2008, 86, 1034-1043.	0.6	17
645	Evaluation Analysis of Prediction Methods for Two-Phase Flow Pressure Drop in Mini-Channels. , 2008, , .		9
646	Octacarbonyl(5-methoxy-2,3-dihydro-1 <i>H</i> -benzimidazol-2-yl)di-μ ₃ -sulfido-diiron(I)iron(II)(2 <i>Acta Crystallographica Section E: Structure Reports Online, 2008, 64, m217-m217.</i>	Fe‒ 0.2	' <i>Fe<∕i>). 4</i>
647	Electrogenerated Chemiluminescence of a Series of Donorâ^'Acceptor Molecules and X-ray Crystallographic Evidence for the Reaction Mechanisms. Journal of Physical Chemistry C, 2007, 111, 9595-9602.	1.5	29
648	Synthesis and photophysical and electrochemical properties of a binuclear Ru (bpy) ₃ - Cu (III) corrole complex. Journal of Porphyrins and Phthalocyanines, 2007, 11, 463-469.	0.4	16

#	Article	IF	CITATIONS
649	Synthesis of 3â€Arylâ€5â€tâ€butylsalicylaldehydes and their Chiral Schiff Base Compounds. Synthetic Communications, 2007, 37, 3815-3826.	1.1	7
650	Influence of ï€-Conjugation Units in Organic Dyes for Dye-Sensitized Solar Cells. Journal of Physical Chemistry C, 2007, 111, 1853-1860.	1.5	160
651	Electronic and Molecular Surface Structure of a Polyeneâ^'Diphenylaniline Dye Adsorbed from Solution onto Nanoporous TiO2. Journal of Physical Chemistry C, 2007, 111, 8580-8586.	1.5	61
652	Synthesis and Electron Transfer Studies of Rutheniumâ^'Terpyridine-Based Dyads Attached to Nanostructured TiO2. Inorganic Chemistry, 2007, 46, 638-651.	1.9	63
653	Fe–S complexes containing five-membered heterocycles: novel models for the active site of hydrogenases with unusual low reduction potential. Dalton Transactions, 2007, , 896-902.	1.6	59
654	Carbene–pyridine chelating 2Fe2S hydrogenase model complexes as highly active catalysts for the electrochemical reduction of protons from weak acid (HOAc). Dalton Transactions, 2007, , 1277-1283.	1.6	85
655	Selective binding of cucurbit[7]uril and β-cyclodextrin with a redox-active molecular triad Ru(bpy)3–MV2+–naphthol. Chemical Communications, 2007, , 4734.	2.2	32
656	Protonation, electrochemical properties and molecular structures of halogen-functionalized diiron azadithiolate complexes related to the active site of iron-only hydrogenases. Dalton Transactions, 2007, , 3812.	1.6	60
657	Intermolecular Electron Transfer from Photogenerated Ru(bpy)3+to [2Fe2S] Model Complexes of the Iron-Only Hydrogenase Active Site. Inorganic Chemistry, 2007, 46, 3813-3815.	1.9	107
658	Hostâ^'Guest Chemistry and Light Driven Molecular Lock of Ru(bpy)3â^'Viologen with Cucurbit[7â^'8]urils. Journal of Physical Chemistry B, 2007, 111, 13357-13363.	1.2	55
659	Binuclear Ironâ^'Sulfur Complexes with Bidentate Phosphine Ligands as Active Site Models of Fe-Hydrogenase and Their Catalytic Proton Reduction. Inorganic Chemistry, 2007, 46, 1981-1991.	1.9	176
660	Iron(III) Complexes with a Tripodal N ₃ O Ligand Containing an Internal Base as a Model for Catechol Intradiol-Cleaving Dioxygenases. Inorganic Chemistry, 2007, 46, 9364-9371.	1.9	38
661	Effect of Tetrahydroquinoline Dyes Structure on the Performance of Organic Dye-Sensitized Solar Cells. Chemistry of Materials, 2007, 19, 4007-4015.	3.2	302
662	Phenothiazine derivatives for efficient organic dye-sensitized solar cells. Chemical Communications, 2007, , 3741.	2.2	446
663	Synthesis and Photophysical and Electrochemical Study of Tyrosine Covalently Linked to High-Valent Copper(III) and Manganese(IV) Complexes. Helvetica Chimica Acta, 2007, 90, 553-561.	1.0	15
664	Phosphane and Phosphite Unsymmetrically Disubstituted Diiron Complexes Related to the Fe-Only Hydrogenase Active Site. European Journal of Inorganic Chemistry, 2007, 2007, 3718-3727.	1.0	32
665	Effect of Deprotonation of a Benzimidazolyl Ligand on the Redox Potential and the Structures of Mononuclear Ruthenium(II) Complexes. European Journal of Inorganic Chemistry, 2007, 2007, 4128-4131.	1.0	5
666	Anthraquinone dyes as photosensitizers for dye-sensitized solar cells. Solar Energy Materials and Solar Cells, 2007, 91, 1863-1871.	3.0	57

#	Article	IF	CITATIONS
667	Synthesis and characterization of manganese and copper corrole xanthene complexes as catalysts for water oxidation. Tetrahedron, 2007, 63, 1987-1994.	1.0	89
668	Synthesis, electrochemical, and photophysical studies of multicomponent systems based on porphyrin and ruthenium(II) polypyridine complexes. Tetrahedron, 2007, 63, 9195-9205.	1.0	12
669	Diiron azadithiolates with hydrophilic phosphatriazaadamantane ligand as iron-only hydrogenase active site models: Synthesis, structure, and electrochemical study. Inorganica Chimica Acta, 2007, 360, 2411-2419.	1.2	39
670	Synthesis, structures and electrochemical properties of hydroxyl- and pyridyl-functionalized diiron azadithiolate complexes. Polyhedron, 2007, 26, 904-910.	1.0	34
671	Preparation, characteristics and crystal structures of novel N-heterocyclic carbene substituted furan- and pyridine-containing azadithiolate Fe–S complexes. Polyhedron, 2007, 26, 1499-1504.	1.0	32
672	Facile and highly efficient light-induced PR3/CO ligand exchange: A novel approach to the synthesis of [(μ-SCH2NnPrCH2S)Fe2(CO)4(PR3)2]. Journal of Organometallic Chemistry, 2007, 692, 1579-1583.	0.8	22
673	Azadithiolates cofactor of the iron-only hydrogenase and its PR3-monosubstituted derivatives: Synthesis, structure, electrochemistry and protonation. Journal of Organometallic Chemistry, 2007, 692, 5501-5507.	0.8	55
674	Tetrahydroquinoline dyes with different spacers for organic dye-sensitized solar cells. Journal of Photochemistry and Photobiology A: Chemistry, 2007, 189, 295-300.	2.0	170
675	Pentacarbonyl-1κ2C,2κ3C-(diphenylphosphine-1κP)(μ-2-propyl-2-azapropane-1,3-dithiolato-1κ2S,Sâ€2:2κ2S,Sâ Acta Crystallographica Section E: Structure Reports Online, 2007, 63, m1959-m1960.	i€²)diiron(0.2	(Fe—Fe). 1
676	Tuning the HOMO and LUMO Energy Levels of Organic Chromophores for Dye Sensitized Solar Cells. Journal of Organic Chemistry, 2007, 72, 9550-9556.	1.7	576
677	Practical Synthesis of New βâ€Diketoneâ€Connected Bipyridine and Its Conversion to Pyrazoleâ€Centered Bipyridine Ligand. Synthetic Communications, 2007, 37, 3393-3402.	1.1	8
678	A Computational Study of Oâ^'O Bond Formation Catalyzed by Mono- and Bis-MnIVâ^'Corrole Complexes. Inorganic Chemistry, 2007, 46, 7075-7086.	1.9	56
679	Preparation, structures and electrochemical property of phosphine substituted diiron azadithiolates relevant to the active site of Fe-only hydrogenases. Journal of Inorganic Biochemistry, 2007, 101, 506-513.	1.5	37
680	Influence of the built-in pyridinium salt on asymmetric epoxidation of substituted chromenes catalysed by chiral (pyrrolidine salen)Mn(III) complexes. Journal of Molecular Catalysis A, 2007, 270, 278-283.	4.8	10
681	Bio-inspired, side-on attachment of a ruthenium photosensitizer to an iron hydrogenase active site model. Dalton Transactions, 2006, , 4599-4606.	1.6	105
682	A wide pH range optical sensing system based on a sol–gel encapsulated amino-functionalised corrole. Analyst, The, 2006, 131, 388.	1.7	60
683	An insight into the protonation property of a diiron azadithiolate complex pertinent to the active site of Fe-only hydrogenases. Chemical Communications, 2006, , 305-307.	2.2	73
684	The photoinduced long-lived charge-separated state of Ru(bpy)3–methylviologen with cucurbit[8]uril in aqueous solution. Chemical Communications, 2006, , 4195-4197.	2.2	46

#	Article	IF	CITATIONS
685	Synthesis of chiral salen Mn(III) complexes covalently linked to Re(I)-based photosensitizers. Journal of Coordination Chemistry, 2006, 59, 475-484.	0.8	1
686	Mono- and binuclear complexes of iron(ii) and iron(iii) with an N4O ligand: synthesis, structures and catalytic properties in alkane oxidation. Dalton Transactions, 2006, , 2427.	1.6	37
687	Bidentate Phosphine Ligand Based Fe2S2-Containing Macromolecules:  Synthesis, Characterization, and Catalytic Electrochemical Hydrogen Production. Inorganic Chemistry, 2006, 45, 9169-9171.	1.9	29
688	A novel organic chromophore for dye-sensitized nanostructured solar cells. Chemical Communications, 2006, , 2245.	2.2	651
689	Asymmetric Oxidation of Sulfides Catalyzed by Vanadium(IV) Complexes of Dibromo- and Diiodo-Functionalized Chiral Schiff Bases. Chinese Journal of Catalysis, 2006, 27, 743-748.	6.9	22
690	The bromination mechanism of 1-aminoanthraquinone-2,4-disulfonic acid in sulfuric acid. Dyes and Pigments, 2006, 71, 231-235.	2.0	3
691	A furan-containing diiron azadithiolate hexacarbonyl complex with unusual lower catalytic proton reduction potential. Inorganic Chemistry Communication, 2006, 9, 290-292.	1.8	41
692	A new, dinuclear high spin manganese(III) complex with bridging phenoxy and methoxy groups. Structure and magnetic properties. Inorganic Chemistry Communication, 2006, 9, 1195-1198.	1.8	11
693	Synthesis, structures and electrochemical properties of amino-derivatives of diiron azadithiolates as active site models of Fe-only hydrogenase. Inorganica Chimica Acta, 2006, 359, 1071-1080.	1.2	31
694	Asymmetric epoxidation of styrene and chromenes catalysed by dimeric chiral (pyrrolidine) Tj ETQq0 0 0 rgBT /O	verlock 10 2.2) Tf 50 382 Tc 19
695	An approach to water-soluble hydrogenase active site models: Synthesis and electrochemistry of diiron dithiolate complexes with 3,7-diacetyl-1,3,7-triaza-5-phosphabicyclo[3.3.1]nonane ligand(s). Journal of Organometallic Chemistry, 2006, 691, 5045-5051.	0.8	66
696	Sign of excited spin state magnetic anisotropy parameters. Spectrochimica Acta - Part A: Molecular and Biomolecular Spectroscopy, 2006, 63, 541-543.	2.0	1
697	A novel ruthenium(II) tris(bipyridine)–zinc porphyrin–rhenium carbonyl triad: synthesis and optical properties. Tetrahedron, 2006, 62, 3674-3680.	1.0	13
698	Donor–acceptor molecules containing thiophene chromophore: synthesis, spectroscopic study and electrogenerated chemiluminescence. Tetrahedron Letters, 2006, 47, 4961-4964.	0.7	16
699	Aryl-diamide bridged binuclear ruthenium (II) tris(bipyridine) complexes: Synthesis, photophysical, electrochemical and electrochemiluminescence properties. Journal of Organometallic Chemistry, 2006, 691, 4189-4195.	0.8	19
700	Asymmetric epoxidation of styrene and chromenes catalysed by chiral (salen)Mn(III) complexes with a pyrrolidine backbone. Journal of Catalysis, 2006, 237, 248-254.	3.1	30
701	Asymmetric oxidation of sulfides catalyzed by chiral (salen)Mn(III) complexes with a pyrrolidine backbone. Applied Organometallic Chemistry, 2006, 20, 830-834.	1.7	23
702	Synthesis of some new 4â€substitutedâ€3, 5â€bis(2â€pyridyl)â€1 <i>h</i> â€pyrazole. Journal of Heterocyclic Chemistry, 2006, 43, 1669-1672.	1.4	4

#	Article	IF	CITATIONS
703	Preparation and structures of 6- and 7-coordinate salen-type zirconium complexes and their catalytic properties for oligomerization of ethylene. Journal of Organometallic Chemistry, 2005, 690, 3929-3936.	0.8	31
704	Synthesis, characterization and some properties of amide-linked porphyrin–ruthenium(II) tris(bipyridine) complexes. Tetrahedron, 2005, 61, 5655-5662.	1.0	28
705	Synthesis and property of a chiral salen Mn(III) complex covalently linked to an Ru(II) tris(bipyridyl) photosensitizer. Inorganic Chemistry Communication, 2005, 8, 606-609.	1.8	10
706	Iron hydrogenase active site mimics in supramolecular systems aiming for light-driven hydrogen production. Coordination Chemistry Reviews, 2005, 249, 1653-1663.	9.5	267
707	Influence of Tertiary Phosphanes on the Coordination Configurations and Electrochemical Properties of Iron Hydrogenase Model Complexes: Crystal Structures of [(μ-S2C3H6)Fe2(CO)6-nLn] (L =) Tj ET	Qq 1 .đ 0.7	84 316 rgBT
708	An Unusual Cyclization in a Bis(cysteinyl-S) Diiron Complex Related to the Active Site of Fe-Only Hydrogenases. Angewandte Chemie - International Edition, 2005, 44, 506-506.	7.2	0
709	Synthesis and Characterization of Dinuclear Ruthenium Complexes Covalently Linked to Rull Tris-bipyridine: An Approach to Mimics of the Donor Side of Photosystem II. Chemistry - A European Journal, 2005, 11, 7305-7314.	1.7	39
710	Synthesis, Structures and Electrochemical Properties of Nitro- and Amino-Functionalized Diiron Azadithiolates as Active Site Models of Fe-Only Hydrogenases. Chemistry - A European Journal, 2005, 11, 803-803.	1.7	0
711	Coordination polyhedra of eight-coordinate zirconium complexes and a network built up by crisscross ClCl contacts. Transition Metal Chemistry, 2005, 30, 517-522.	0.7	8
712	Pentacarbonyl(diphenyl(N-propylamine)phosphine)diiron(μ-1,3-propanedithiolate). Acta Crystallographica Section E: Structure Reports Online, 2005, 61, m852-m853.	0.2	1
713	Axial ligand exchange reaction on ruthenium phthalocyanines. Journal of Porphyrins and Phthalocyanines, 2005, 09, 248-255.	0.4	10
714	Spectroscopic and crystallographic evidence for the N-protonated FelFel azadithiolate complex related to the active site of Fe-only hydrogenases. Chemical Communications, 2005, , 3221.	2.2	49
715	Synthesis and redox properties of a [<i>meso</i> -tris(4-nitrophenyl) corrolato] Mn(III) complex. Journal of Porphyrins and Phthalocyanines, 2005, 09, 379-386.	0.4	20
716	A New Strategy for the Improvement of Photophysical Properties in Ruthenium(II) Polypyridyl Complexes. Synthesis and Photophysical and Electrochemical Characterization of Six Mononuclear Ruthenium(II) Bisterpyridine-Type Complexes. Inorganic Chemistry, 2005, 44, 3215-3225.	1.9	97
717	Switching the Redox Mechanism:Â Models for Proton-Coupled Electron Transfer from Tyrosine and Tryptophan. Journal of the American Chemical Society, 2005, 127, 3855-3863.	6.6	224
718	A Biomimetic Pathway for Hydrogen Evolution from a Model of the Iron Hydrogenase Active Site. Angewandte Chemie - International Edition, 2004, 43, 1006-1009.	7.2	232
719	An Unusual Cyclization in a Bis(cysteinyl-S) Diiron Complex Related to the Active Site of Fe-Only Hydrogenases. Angewandte Chemie - International Edition, 2004, 43, 3571-3574.	7.2	26
720	Preparation, characterization and catalytic oxidation properties of tris[2-(2-pyridyl)benzimidazole]iron(II) complexes. Applied Organometallic Chemistry, 2004, 18, 277-281.	1.7	2

#	Article	IF	CITATIONS
721	Synthesis, Structural Characterizations and Magnetic Properties of a Series of Mono-, Di- and Polynuclear Manganese Pyridinecarboxylate Compounds. European Journal of Inorganic Chemistry, 2004, 2004, 1454-1464.	1.0	66
722	Synthesis, Structure and Magnetic Properties of a Series of Novel Isophthalate-Bridged Manganese(II) Polymers with Double-Layer or Double-Chain Structures. European Journal of Inorganic Chemistry, 2004, 2004, 3316-3325.	1.0	45
723	Synthesis, Structures and Electrochemical Properties of Nitro- and Amino-Functionalized Diiron Azadithiolates as Active Site Models of Fe-Only Hydrogenases. Chemistry - A European Journal, 2004, 10, 4474-4479.	1.7	83
724	Effects of the precatalyst structure and the Mg-containing third-component on cyclo-oligomerization of ethene. Journal of Molecular Catalysis A, 2004, 216, 13-17.	4.8	4
725	Novel porphyrin–thallium–platinum complex with "naked―metal–metal bond: multinuclear NMR characterization of [(tpp)Tl–Pt(CN)5]2â^' and [(thpp)Tl–Pt(CN)5]2â^' in solution. Inorganica Chimica Acta, 2004, 357, 4073-4077.	1.2	6
726	Salen-type zirconium complexes with a labile coordination site and a robust skeleton: crystal structure of [(t-Bu4-salen)ZrCl2(H2O)]. Journal of Organometallic Chemistry, 2004, 689, 1212-1217.	0.8	17
727	Light-induced multistep oxidation of dinuclear manganese complexes for artificial photosynthesis. Journal of Inorganic Biochemistry, 2004, 98, 733-745.	1.5	36
728	A tridentate ligand for preparation of bisterpyridine-like ruthenium(II) complexes with an increased excited state lifetime. Inorganic Chemistry Communication, 2004, 7, 337-340.	1.8	37
729	Synthesis of a Ru(bpy)3-type complex linked to a free terpyridine ligand and its use for preparation of polynuclear bimetallic complexes. Catalysis Today, 2004, 98, 529-536.	2.2	23
730	Tuning proton coupled electron transfer from tyrosine: A competition between concerted and step-wise mechanisms. Physical Chemistry Chemical Physics, 2004, 6, 4851-4858.	1.3	72
731	Intramolecular charge separation in a hydrogen bonded tyrosine–ruthenium(ii)–naphthalene diimide triad. Chemical Communications, 2004, , 194-195.	2.2	34
732	Model of the Iron Hydrogenase Active Site Covalently Linked to a Ruthenium Photosensitizer:Â Synthesis and Photophysical Properties. Inorganic Chemistry, 2004, 43, 4683-4692.	1.9	136
733	Carotenoid and Pheophytin on Semiconductor Surface:  Self-Assembly and Photoinduced Electron Transfer. Journal of the American Chemical Society, 2004, 126, 3066-3067.	6.6	45
734	Stepwise Charge Separation from a Rutheniumâ^'Tyrosine Complex to a Nanocrystalline TiO2Film. Journal of Physical Chemistry B, 2004, 108, 12904-12910.	1.2	28
735	Synthesis of phthalocyanines with two carboxylic acid groups and their utilization in solar cells based on nano-structured TiO ₂ . Journal of Porphyrins and Phthalocyanines, 2004, 08, 1228-1235.	0.4	33
736	Synthesis and Characterisation of a High Valent Dinuclear Mn(III,III) Complex of a Triphenolate Ligand [N4O3]3- with two Extra Functional Groups. Journal of Chemical Research, 2004, 2004, 57-58.	0.6	0
737	Electrospray Ionization Mass Spectrometry Studies of Rhenium(I) Bipyridyl Complexes. European Journal of Mass Spectrometry, 2004, 10, 599-603.	0.5	2
738	Electron Donorâ^'Acceptor Dyads and Triads Based on Tris(bipyridine)ruthenium(II) and Benzoquinone: Synthesis, Characterization, and Photoinduced Electron Transfer Reactions. Inorganic Chemistry, 2003, 42, 5173-5184.	1.9	65

#	Article	IF	CITATIONS
739	Ethylene oligomerization by salen-type zirconium complexes to low-carbon linear α-olefins. Journal of Catalysis, 2003, 220, 392-398.	3.1	55
740	Great Framework Variation of Polymers in the Manganese(II) Maleate/α,α′-Diimine System: Syntheses, Structures, and Magneto-Structural Correlation. European Journal of Inorganic Chemistry, 2003, 2003, 2872-2879.	1.0	28
741	Title is missing!. Angewandte Chemie, 2003, 115, 3407-3410.	1.6	39
742	Synthesis of an Amino-Functionalized Model of the Fe-Only Hydrogenase Active Site. Chemistry - A European Journal, 2003, 9, 557-560.	1.7	33
743	Synthesis and Structure of a Biomimetic Model of the Iron Hydrogenase Active Site Covalently Linked to a Ruthenium Photosensitizer. Angewandte Chemie - International Edition, 2003, 42, 3285-3288.	7.2	191
744	Synthesis, structural characterization and magnetic properties of 2-pyrazinecarboxylate manganese compounds [Mn(pyz)2(H2O)4] and [MnCl(pyz)(H2O)]n (pyz=2-pyrazinecarboxylate). Inorganica Chimica Acta, 2003, 353, 284-291.	1.2	24
745	Synthesis and properties of an iron hydrogenase active site model linked to a ruthenium tris-bipyridine photosensitizer. Inorganic Chemistry Communication, 2003, 6, 989-991.	1.8	58
746	catena-Poly[[[(1,10-phenanthroline-κ2N,N′)manganese(II)]-μ-L-tartrato-κ4O1,O2:O3,O4] hexahydrate]. Acta Crystallographica Section C: Crystal Structure Communications, 2003, 59, m402-m404.	0.4	2
747	Aggregate Manganese Schiff Base Moieties by Terephthalate or Acetate:  Dinuclear Manganese and Trinuclear Mixed Metal Mn2/Na Complexes. Inorganic Chemistry, 2003, 42, 3540-3548.	1.9	41
748	Mixed-Valence Properties of an Acetate-Bridged Dinuclear Ruthenium (II,III) Complex. Journal of Physical Chemistry A, 2003, 107, 4373-4380.	1.1	10
749	Determination of EDTA species in water by square-wave voltammetry using a chitosan-coated glassy carbon electrode. Water Research, 2003, 37, 4270-4274.	5.3	13
750	Electron Donorâ^'Acceptor Dyads Based on Ruthenium(II) Bipyridine and Terpyridine Complexes Bound to Naphthalenediimide. Inorganic Chemistry, 2003, 42, 2908-2918.	1.9	112
751	Synthesis and Photophysics of One Mononuclear Mn(III) and One Dinuclear Mn(III,III) Complex Covalently Linked to a Ruthenium(II) Tris(bipyridyl) Complex. Inorganic Chemistry, 2003, 42, 7502-7511.	1.9	38
752	Structural transformation mediated by o-, m-, and p-phthalates from two to three dimensions for manganese/phthalate/4,4′-bpy complexes (4,4′-bpy = 4,4′-bipyridine). New Journal of Chemistry, 890-894.	2003, 27	', 95
753	Toward Solar Energy Conversion into Fuels: Design and Synthesis of Ruthenium—Manganese Supramolecular Complexes to Mimic the Function of Photosystem II. ACS Symposium Series, 2003, , 219-244.	0.5	1
754	Determination of EDTA Species in Water by Second-Derivative Square-Wave Voltammetry Using a Chitosan-Coated Glassy Carbon Electrode. Analytical Sciences, 2003, 19, 607-609.	0.8	7
755	Ruthenium phthalocyanines with axial carboxylate ligands: Synthesis and function in solar cells based on nanocrystalline TiO ₂ . Journal of Porphyrins and Phthalocyanines, 2002, 06, 217-224.	0.4	32
756	Electron, proton and hydrogen–atom transfers in photosynthetic water oxidation. Philosophical Transactions of the Royal Society B: Biological Sciences, 2002, 357, 1383-1394.	1.8	38

#	Article	IF	CITATIONS
757	The mechanism for proton–coupled electron transfer from tyrosine in a model complex and comparisons with Y Z oxidation in photosystem II. Philosophical Transactions of the Royal Society B: Biological Sciences, 2002, 357, 1471-1479.	1.8	54
758	XPS and UPS Characterization of the TiO2/ZnPcGly Heterointerface:Â Alignment of Energy Levels. Journal of Physical Chemistry B, 2002, 106, 5814-5819.	1.2	191
759	Rutheniumâ^'Manganese Complexes for Artificial Photosynthesis:Â Factors Controlling Intramolecular Electron Transfer and Excited-State Quenching Reactions. Inorganic Chemistry, 2002, 41, 1534-1544.	1.9	82
760	Light-Driven Tyrosine Radical Formation in a Rutheniumâ^'Tyrosine Complex Attached to Nanoparticle TiO2. Inorganic Chemistry, 2002, 41, 6258-6266.	1.9	35
761	Photoinduced Electron Transfer between a Carotenoid and TiO2Nanoparticle. Journal of the American Chemical Society, 2002, 124, 13949-13957.	6.6	94
762	Modified Phthalocyanines for Efficient Near-IR Sensitization of Nanostructured TiO2 Electrode. Journal of the American Chemical Society, 2002, 124, 4922-4932.	6.6	396
763	Synthesis, Redox Properties, and EPR Spectroscopy of Manganese(III) Complexes of the Ligand N,N-Bis(2-hydroxybenzyl)-Nâ€2-2-hydroxybenzylidene-1,2-diaminoethane: Formation of Mononuclear, Dinuclear, and Even Higher Nuclearity Complexes. Chemistry - A European Journal, 2002, 8, 3757.	1.7	29
764	Synthesis and Characterization of a Dinuclear Manganese(III,III) Complex with Three Phenolate Ligands. European Journal of Inorganic Chemistry, 2002, 2002, 2965-2974.	1.0	47
765	Photo-induced oxidation of a dinuclear Mn2II,II complex to the Mn2III,IV state by inter- and intramolecular electron transfer to RullItris-bipyridine. Journal of Inorganic Biochemistry, 2002, 91, 159-172.	1.5	97
766	Synthesis and Characterization of a Dinuclear Manganese(III,III) Complex with Three Phenolate Ligands. , 2002, 2002, 2965.		1
767	LIGHT DRIVEN MULTISTEP ELECTRON TRANSFER IN A TYROSINE-RUTHENIUM-COMPLEX ANCHORED TO TIO ₂ NANOPARTICLES. , 2002, , .		0
768	Phthalocyanine-Sensitized Nanostructured TiO2Electrodes Prepared by a Novel Anchoring Method. Langmuir, 2001, 17, 2743-2747.	1.6	124
769	A biomimetic approach to artificial photosynthesis: Ru(II)–polypyridine photo-sensitisers linked to tyrosine and manganese electron donors. Spectrochimica Acta - Part A: Molecular and Biomolecular Spectroscopy, 2001, 57, 2145-2160.	2.0	35
770	Covalently Linked Ruthenium(II)â^'Manganese(II) Complexes: Distance Dependence of Quenching and Electron Transfer. European Journal of Inorganic Chemistry, 2001, 2001, 1019-1029.	1.0	65
771	Towards artificial photosynthesis: ruthenium–manganese chemistry for energy production. Chemical Society Reviews, 2001, 30, 36-49.	18.7	530
772	Covalently Linked Ruthenium(II)â^'Manganese(II) Complexes: Distance Dependence of Quenching and Electron Transfer. European Journal of Inorganic Chemistry, 2001, 2001, 1019-1029.	1.0	3
773	Mimicking photosystem II reactions in artificial photosynthesis: Ru(II)-polypyridine photosensitisers linked to tyrosine and manganese electron donors. Catalysis Today, 2000, 58, 57-69.	2.2	14
774	Towards an artificial model for Photosystem II: a manganese(II,II) dimer covalently linked to ruthenium(II) tris-bipyridine via a tyrosine derivative1Preliminary accounts of this work have been presented as invited lectures at: EUCHEM Conference, Artificial Photosynthesis, May 1998, Sigtuna, Sweden; Fourth Nordic Congress on Photosynthesis, Nov. 1998, Naantali, Finland; EBEC, July 1998, Göteborg, Sweden.1. Journal of Inorganic Biochemistry, 2000, 78, 15-22.	1.5	73

#	Article	IF	CITATIONS
775	Proton-Coupled Electron Transfer from Tyrosine in a Tyrosineâ^'Rutheniumâ^'tris-Bipyridine Complex:Â Comparison with TyrosineZOxidation in Photosystem II. Journal of the American Chemical Society, 2000, 122, 3932-3936.	6.6	262
776	Photoinduced Electron Transfer from a Higher Excited State of a Porphyrin in a Zinc Porphyrinâ^'Ruthenium(II)tris-Bipyridine Dyad. Journal of Physical Chemistry A, 1999, 103, 557-559.	1.1	88
777	A Biomimetic Model System for the Water Oxidizing Triad in Photosystem II. Journal of the American Chemical Society, 1999, 121, 89-96.	6.6	75
778	Hydrogen-Bond Promoted Intramolecular Electron Transfer to Photogenerated Ru(III):  A Functional Mimic of TyrosineZ and Histidine 190 in Photosystem II. Journal of the American Chemical Society, 1999, 121, 6834-6842.	6.6	90
779	Artificial photosynthesis: Towards functional mimics of photosystem II?. Biochimica Et Biophysica Acta - Bioenergetics, 1998, 1365, 193-199.	0.5	15
780	Intramolecular Electron Transfer from Manganese(II) Coordinatively Linked to a Photogenerated Ru(III)â^Polypyridine Complex:  A Kinetic Analysis. Journal of Physical Chemistry A, 1998, 102, 2512-2518.	1.1	38
781	Light-Induced Electron Transfer Between A Substituted Tyrosine and [Ru(bpy)3]2+. , 1998, , 4217-4220.		0
782	Intramolecular electron transfer from coordinated manganese(ii) to photogenerated ruthenium(iii). Chemical Communications, 1997, , 607-608.	2.2	37
783	Mimicking Electron Transfer Reactions in Photosystem II:  Synthesis and Photochemical Characterization of a Ruthenium(II) Tris(bipyridyl) Complex with a Covalently Linked Tyrosine. Journal of the American Chemical Society, 1997, 119, 10720-10725.	6.6	135
784	Binuclear Rutheniumâ^'Manganese Complexes as Simple Artificial Models for Photosystem II in Green Plants. Journal of the American Chemical Society, 1997, 119, 6996-7004.	6.6	123
785	Towards artificial photosynthesis — Light-induced intramolecular electron transfer from manganese (II) to ruthenium (III) in a binuclear complex. Journal of Chemical Sciences, 1997, 109, 389-396.	0.7	2
786	Time-resolved EPR studies of covalently linked porphyrin—crown ether—quinones, dissolved in liquid crystals. Magnetic Resonance in Chemistry, 1995, 33, S28-S33.	1.1	11
787	Novel biomimetic models for photosynthesis: Porphyrins covalently linked to redox-active crown ether quinones. Tetrahedron, 1995, 51, 3535-3548.	1.0	23
788	Mimicking primary processes in photosynthesis photochemistry of covalently linked porphyrin quinones studied by EPR spectroscopy. Solar Energy Materials and Solar Cells, 1995, 38, 91-110.	3.0	15
789	Fluorescence quenching of viologen on xanthene dyes in dyads. Dyes and Pigments, 1995, 28, 275-279.	2.0	3
790	Inhibition of OH Radical-induced Strand Break Formation of Poly(U) by Ru(bpy) ²⁺ ₃ or Ru(phen) ²⁺ ₃ Attached to the Polynucleotide. International Journal of Radiation Biology, 1995, 68, 525-533.	1.0	0
791	Biomimetic Model for a Photosynthetic Reaction Center: A Porphyrin with a Covalently Linked, Redox-Active Crown Ether. Angewandte Chemie International Edition in English, 1994, 33, 2318-2320.	4.4	34
792	Biomimetische Modelle für das photosynthetische Reaktionszentrum: ein kovalent mit einem redoxaktiven Kronenether verknüpftes Porphyrin. Angewandte Chemie, 1994, 106, 2396-2399.	1.6	11

#	Article	IF	CITATIONS
793	Trans → cis photoisomerization of 1-(9-anthryl)-2-(4-R-phenyl)ethylene, R: CH3 and OCH3. Chemical Physics Letters, 1993, 208, 43-47.	1.2	15
794	Excited-state properties of trans-1-(9-anthryl)-2-(4-R-phenyl)ethylenes with electron-donating and -accepting substituents [R = N(CH3)2, OCH3, CH3, Br, CN, and NO2]. The Journal of Physical Chemistry, 1993, 97, 11186-11193.	2.9	23
795	Phenanthrocarbazoleâ€Based Dopantâ€Free Holeâ€Transport Polymer with Noncovalently Conformational Locking for Efficient Perovskite Solar Cells. Angewandte Chemie, 0, , .	1.6	3
796	Pyreneâ€Based Dopantâ€Free Holeâ€Transport Polymers with Fluorine Induced Favorable Molecular Stacking Enable Efficient Perovskite Solar Cells. Angewandte Chemie, 0, , .	1.6	4